key words:
1- shear tabs
2- tubular conn's

3488 No. Cramer Street
Milwaukee, WI 53211
January 11, 1990

Mr. Nestor Iwankiw
American Institute of Steel Const.
The Wrigley Building - Eigth Floor
400 North Michigan Avenue
Chicago, IL 60611-4185

Dear Mr. Iwankiw:

Enclosed you will find a copy of my thesis entitled "The Effect of Shear Tab Connections on Tubular Column Strengths." This thesis is the final report on the results of my graduate project. If you have any questions regarding this final report call me at 414-351-5588. Once again I would like to thank you and the AISC Education Foundation for awarding me one of the fellowships in 1986.

Sincerely,

Stephen M. Herlache

Stephen M. Herlache

Enclosure

The Effect of Shear Tab Connections on Tubular Column Strengths

By

Stephen Michael Herlache

A Thesis Submitted in
Partial Fulfillment of the
Requirements for the Degree of

Master of Science

Civil Engineering

at

The University of Wisconsin-Milwaukee

December, 1989

The Effect of Shear Tab Connections on Tubular Column Strengths

By

Stephen Michael Herlache

A Thesis Submitted in
Partial Fulfillment of the
Requirements for the Degree of

Master of Science

Civil Engineering

at

The University of Wisconsin-Milwaukee

December , 1989

D. R. Sherman — 9/28/89
Major Professor — Date

George W. Kreutzer — 11-13-89
Graduate School Approval — Date

The Effect of Shear Tab Connections on Tubular Column Strengths

By

Stephen Michael Herlache

The University of Wisconsin - Milwaukee, 1989
Under the Supervision of Donald R. Sherman

Single plate framing connections, also known as shear tabs, are becoming popular in the steel building industry due to their savings in fabrication and erection costs. These shear tabs are readily accepted by engineers when used with I-shaped columns under light loads due to design recommendations suggested by recent research. However, the capacity of tubular columns has been questioned if shear tabs are welded to their walls, causing local distortions.

At the University of Wisconsin - Milwaukee a pilot study of four full-scale column tests was conducted to see how tubular columns behave with shear tabs welded to their walls. The test specimens of this investigation consisted of two control columns and two test columns. The control group was comprised of two rectangular-tubular columns with through plate connections that have the erection advantages of the shear tab but also reinforce the wall. The through plate connection is often specified by designers in place of

the shear tab due to uncertainties of their effect on tubular column strength. The test group consisted of rectangular-tubular columns with shear tabs welded to the walls. Furthermore, in one of the specimens in each group, the bolts were snug-tight and in the other pair, they were fully tightened as in a slip control connection.

The results of the four tests indicated the following: (1) the capacity of rectangular-tubular columns with shear tabs welded to its walls were within 4 percent of the capacities for the tubular columns with the through plate connection, (2) based on beam-line theory the shear tab connection performed as a simple "Type 2" connection even with the through plate connection, and (3) there was a significant increase in transverse strain in the tubular columns with shear tabs in comparison with the tubular columns with through plates.

D. R. Sherman — 9/28/89

Major Professor — Date

TABLE OF CONTENTS

LIST OF TABLES

LIST OF FIGURES

1. INTRODUCTION

1.1 General

The use of hollow structural sections, circular or rectangular, in the building industry has increased in recent years due to the advantages that they have over other structural shapes. Hollow structural sections have: a high resistance to lateral-torsional buckling; a high torsional strength; and low maintenance requirements when used for exposed structures. More important, hollow structural sections are primarily used as compression members due to their closely matched moments of inertia about the principal axes.

A major concern when using hollow structural sections as column elements is with the intermediate framing connections that are used to attach I-shaped beams to their walls as in multistory framing systems. Due to the inaccessible interior of tubular columns these connections may become complex even for simple "Type 2" connections.

However, recent research [1] has demonstrated that single plate framing connections are adequate in the design of simple "Type 2" connections when welded in line with the web of I-shaped columns. This connection consists of a plate, with pre-punched holes, welded to the flange of an I-shaped column as shown in Figure 1.1. The single plate framing connection, also known as the shear tab connection, provides most of its flexibility through the distortion of

the bolt holes in the connection plate and/or the beam web. The primary advantage of this connection is that field-bolt erection can be used without coping framing beams. Design procedures have been developed to limit the bending in the tab that exists due to the load pattern.

However, the use of shear tab connections in conjunction with tubular columns has been questioned since the capacity of the column may be reduced due to the local wall distortion that exists when I-shaped beams are connected to its face through this narrow connection. An expensive through plate connection is often specified to reinforce the walls of the tubular column. Although this problem has been of concern for the past decade, there has not been any full-scale testing conducted to determine if the column capacity is in fact reduced. Therefore, it is necessary to determine the effect of shear tab connections on tubular column strengths.

1.2 Objectives

The primary objective of this investigation is to determine if the capacity of rectangular-tubular columns is greatly affected when shear tabs are used to connect I-beams to their walls. When loaded, shear tabs produce a local distortion in the wall of tubular columns because the load is delivered to the center of the face of the column instead of near its sidewalls. The severity of this distortion may or may not affect the capacity of these columns.

In addition to the column study, a connection investigation was sought to obtain the moment-rotation characteristics of shear tabs that are welded to tubular columns. With the use of beam lines the flexibility of the connection can be compared to the moment-rotation characteristics of simple "Type 2" connections.

1.3 Scope

Due to the availability of funding, this investigation is considered as a limited pilot study. The test program consisted of four rectangular-tubular columns with a nominal yield strength of 46 ksi. The specimens chosen were selected to best represent the size of tubular columns that are used in the building industry and to conform with the limits of the testing facility.

This paper presents and discusses the results of the four tests that were conducted at the University of Wisconsin-Milwaukee. The test data for each of the four tests is tabulated in Appendix E of this paper for further consultation.

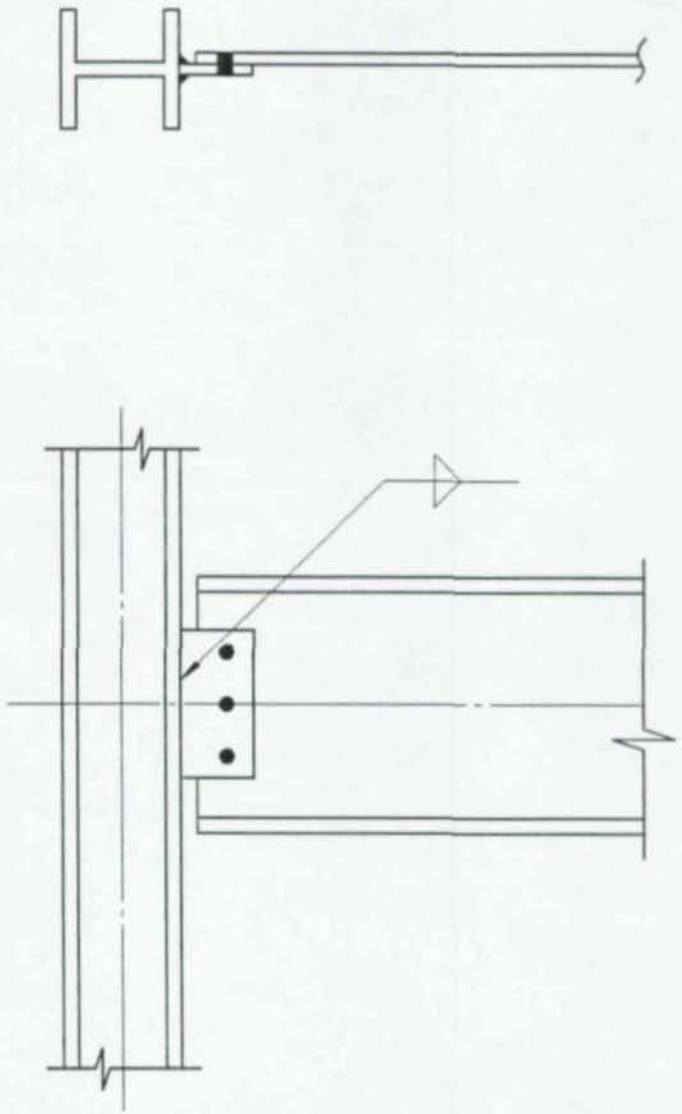

Figure 1.1: Shear Tab Connection

2. RELEVANT STRUCTURAL THEORY

2.1 Basic Column Strength

2.1.1 Elastic Buckling Theory

In order to determine the elastic strength of an "ideal" column the following conditions are assumed: the section is homogeneous and prismatic; small deflection theory is valid; the column is initially straight; the load resultant acts through the centroidal axis of the column until bending due to buckling occurs; twisting or cross section distortion does not occur; no internal residual stresses are present in the section; the end conditions are determinant; and the material remains elastic. With these assumptions, Euler buckling theory determines that the critical buckling load of an "ideal" column can be expressed as

$$P_{cr} = \pi^2 EI/L^2 \qquad (2.1)$$

and the average critical stress in the section is

$$F_{cr} = P_{cr}/A_g$$
$$= \pi^2 E/(L/r)^2 \qquad (2.2)$$

where A_g = gross area of the section,

I = moment of inertia of the section,

E = Young's modulus of elasticity, and

L/r = slenderness ratio.

Euler's buckling equation primarily governs the compressive strength of members with large slenderness ratios. However, for shorter columns, the compressive strength is less than that computed using Eqn. 2.2. Columns of this sort tend to fail inelastically[2,3,4,5,6].

2.1.2 Inelastic Buckling Theory

For long columns the applied axial load reaches the Euler buckling load before the axial stress exceeds the proportional limit of the material. However, for short columns the axial stress may exceed the proportional limit before the applied axial load reaches the Euler buckling load. Therefore, an inelastic approach should be used to determine the buckling strength of short columns.

One of the approaches used to predict the behavior of columns in the inelastic range is the tangent-modulus method. The basic assumptions in the tangent-modulus method are that the applied axial load increases during the transition from stable equilibrium to neutral equilibrium and that there is no strain reversal in the section on the convex side of the slightly deformed column. Therefore, the compressive stress increases for all fibers in the cross section and the stress-strain relationship is governed by the tangent modulus. With this in mind, the critical buckling load at which the column is slightly bent is expressed as

$$P_{cr} = \pi^2 E_t I/L^2 \qquad (2.3)$$

and the average critical stress is

$$F_{cr} = \pi^2 E_t/(L/r)^2 \qquad (2.4)$$

where E_t = tangent modulus.

However, Eqns. 2.3 and 2.4 cannot be used to determine the inelastic buckling strength of steel columns if the stress-strain relationship is obtained from a small coupon cut from the cross section. The coupon is relatively free of residual stress which results in a linear stress-strain relationship up to yielding. The stress-strain relationship of the cross section depends on the yield strength of the material and the magnitude and distribution of residual stresses.

The magnitude and distribution of residual stresses in hot-rolled shapes depend on the shape of the cross section, the initial rolling temperature, the cooling conditions, and the material properties. The residual stress distribution for a particular shape can be determined by the method of sections or it can be estimated from the results of a stub-column test.

The influence of residual stress on the stress-strain curve of a stub column is shown by the solid line in Figure 2.1. Also shown in this figure is the stress-strain curve of a small coupon cut from the cross section. Local

yielding of the cross section will occur if the stub column is loaded in a manner at which the applied axial stress is equal to the yield stress minus the maximum compressive residual stress. As the section is loaded further the stress-strain curve is no longer proportional as shown in Figure 2.1. The slope of a tangent line at any point along this portion of the curve is known as the tangent modulus. Furthermore, the point at which the section begins to yield is known as the effective proportional limit and is defined as

$$F_p = F_y - F_{rc} \qquad (2.5)$$

where F_p = effective proportional limit,

F_y = yield stress, and

F_{rc} = maximum compressive residual stress.

Stress-strain curves can be calculated for doubly-symmetric columns for an assumed symmetrical residual stress distribution and yield stress if stub-column test results are not available. Assuming a uniform yield strength and strain hardening is neglected the tangent modulus can be defined as

$$E_t = dF/d\epsilon = E(A_e/A) \qquad (2.6)$$

where E_t = tangent modulus,

F = average stress,

ϵ = strain,

E = elastic modulus,

A = gross area, and

A_e = area that has not yielded.

When a portion of the stub column has yielded the average stress in the section is

$$F_{av} = (A-A_e)F_y/A + 1/A \int_{Ae} FdA \qquad (2.7)$$

By selecting values of A_e/A between zero and one E_t and F_{av} can be determined from Eqns. 2.6 and 2.7. From the values of E_t and F_{av} slenderness ratios can be determined from Eqn. 2.4 for a pinned column. The column strength curve for the cross section can then be generated from the slenderness ratios and average stresses determined above.

The magnitude of residual stress does not need to be known in the determination of the theoretical column curve since yielding of the cross section is dependent on the A_e/A ratio in Eqns. 2.6 and 2.7. However, the residual stress distribution is necessary to determine the function of A_e/A in the cross section. Therefore, the magnitude of the residual stress does not need to be known if for every shape there is a column curve for a particular residual stress distribution and yield strength.

Another factor that affects the column curve is the initial out-of-straightness of the column. As with residual

stresses, initial out-of-straightness also reduces the capacity of short columns. The affects of residual stress and initial out-of-straightness on the column curve differ for various sections. However, column curves can be obtained experimentally or by computer simulation for an assumed residual stress distribution, yield strength, and initial out-of-straightness. Design curves are somewhat arbitrary averages of several column curves[2,3,4,5,6].

2.1.3 Effective Length Factor

In order to predict the strength of columns with other than pinned ends an effective length factor, K, must be determined. The effective length factor is defined as the ratio of the distance between the points of inflection and the actual length of the member. For example, a pinned-end column has an effective length factor of 1.0 while a fixed-end column has theoretical effective length factor of 0.5. In general, the effective length factor for columns in framing systems is dependent on whether the frame is braced or unbraced. The effective length factor for columns in braced frames is less than one and greater than one in unbraced frames.

The effective length factor of a braced frame can be determined for columns with constant axial load and determinant end conditions such as a one-story column. However, the problem is more complex for continuous columns

that have intermediate framing connections along their length which produce different axial forces in the segments as in a two-story column. As a result, an elastic instability exists in the column that depends on the end restraints of each segment; the ratio of top axial load to the intermediate applied axial load; the ratio of the lengths of each segment; and the moment of inertia of each segment. The effective length factor for a continuous two-story column can be determined by performing a column stability analysis using flexural stiffness functions modified by an axial force. In this analysis, a stiffness matrix can be constructed for the system as shown in Figure 2.2. The effective length factor of each segment is obtained when the determinant of the stiffness matrix approaches zero[7]. Through a trial and error procedure effective length factors can be determined for various loading conditions. Appendix B contains the procedures used in the determination of the theoretical effective length factors incurred in this investigation.

Effective length factors can also be determined for test columns by using Southwell Plots. A Southwell Plot is the graph of the ratio of center displacement to axial load versus center displacement, δ/P versus δ, as shown in Figure 2.3. The equation for the straight line is:

$$\delta/P = \delta/Q + (a_1)/Q \qquad (2.8)$$

where Q = Euler buckling load,

P = axially applied load,

δ = center displacement, and

a_1 = initial central crookedness[8].

The effective length factor of the column can be determined by substituting the Euler buckling load, Q, in the place of P_{cr} in Eqn. 2.1 and solving for K if a an effective length, KL, is used in place of L. Refer to Appendix C for the derivation of Eqn. 2.8 and the calculation of the experimental effective length factors for each of the four tests.

2.1.4 AISC Design Equations

The American Institute of Steel Construction, AISC, adopted its column strength equations from the basic strength suggested by the Structural Stability Research Council, SSRC (formerly the Column Research Council, CRC) [3].

The SSRC column strength curve is based on the parabolic equation proposed by Bleich[9] using a maximum compressive-residual stress of one half of the yield strength, $F_{rc} = 0.5F_y$. After substituting F_{rc} with $0.5F_y$, Bleich's equation then becomes

$$F_c = F_y - \{(F_y)^2(KL/r)^2\}/4\pi^2E \qquad (2.9)$$

where F_c = column strength,

F_y = yield strength,

KL/r = effective slenderness ratio, and

K = effective length factor.

Based on residual stress tests conducted on five wide-flanged sections, cited in Reference 2, the average maximum compressive-residual stress is approximately $0.3F_y$ for ASTM A36 steel. The maximum compressive-residual stress of $0.5F_y$ was used in Bleich's equation so that a smooth transition from Euler's buckling equation and Bleich's equation would occur.

In the AISC Specification, the allowable compressive stress used in the design of axially loaded columns with slenderness ratios in the inelastic range is

$$F_a = [1 - (KL/r)^2/2C_c^2]F_y/FS \qquad (2.10)$$

where F_a = allowable axial stress,

$C_c = \sqrt{2\pi^2E/F_y}$, and

$FS = 5/3 + .375(KL/r)/C_c - .125(KL/rC_c)^3$.

This is AISC Equation (1.5-1) for slenderness ratios less than C_c. The term C_c is the slenderness ratio that corresponds to the upper limit of elastic buckling, $0.5F_y$, suggested by SSRC. In other words, the upper limit of

elastic buckling in where AISC Equation (1.5-1) is tangent to Euler's elastic buckling equation.

The allowable compressive stress used in the design of axially loaded columns with slenderness ratios greater than C_c is

$$F_a = \pi^2 E/[(KL/r)^2(FS)] \qquad (2.11)$$

where FS = 23/12.

This is AISC Equation (1.5-2) which is the elastic buckling strength according to Euler theory as presented in Eqn. 2.2[3,4]. Euler's buckling equation, Eqn. 2.2, is modified by the effective length factor, K, for columns with other than pinned ends.

It should be noted that the equations adopted by AISC are the strength curves suggested by SSRC. However, numerous column strength curves can be generated depending upon the expected residual stress distribution, the shape of the section, the axis of bending when the column buckles, and the initial out-of-straightness. The design equations used by SSRC are a selected average of several column stress curves for various residual stress distributions.

2.1.5 Buckling Equations for Rectangular-Tubular Columns

Figure 2.4, reprinted from Reference 10, is a plot of test data for several axially loaded rectangular tubes. In this figure there are two column strength curves, Class A

and Class B, which designate the level of residual stress that can be expected from the manufacturing process. Class A columns are continuously welded tubular sections that are hot formed into final shape or continuously welded cold-formed tubular sections that are stress relieved. On the other hand, Class B columns are continuously welded tubular sections that are cold-formed into final shape. The equation for the curve that represents the data points for Class A tubular columns is

$$F_a = [1-(KL/r)^2/2C_c^2]F_y/FS \qquad (2.12)$$

where $C_c = \sqrt{2\pi^2E/F_y}$

$= 756/\sqrt{F_y}$

$FS = 5/3 + .375(KL/r)/C_c - (KL/r)^3/8C_c^3.$

For Class B tubular columns the equation is

$$F_a = [1-(KL/r)/1.5C_c]F_y/FS \qquad (2.13)$$

where $C_c = \sqrt{3\pi^2E/F_y}$

$= 925/\sqrt{F_y}$

$FS = 5/3 + (KL/r)/4C_c.$

Equations 2.12 and 2.13 are valid when the flat width to thickness ratio of the longest side does not exceed $238/\sqrt{F_y}$ and the effective slenderness ratio, KL/r, does not exceed C_c. When KL/r exceeds C_c but does not exceed 200, the modified form of Euler's elastic buckling equation, Eqn. 2.11, governs. Furthermore, if the flat width to thickness ratio of any side exceeds $238/\sqrt{F_y}$, then Appendix C of the AISC Specification should be used in conjunction with Eqns. 2.11 and 2.12 or 2.13 to determine the allowable compressive axial stress. Appendix C of the AISC Specification contains the reduction factors for slender compression elements in the column section[3,10].

2.2 Shear Tab Theory

The shear tab connection is a flexible connection that is economical in both the fabrication and erection of steel buildings. The shear tab shown in Figure 1.1 consists of a single plate, with pre-punched holes, that is welded to the supporting element. Shear tabs may also be used to connect beams to the web of a supporting beam.

In the analysis of this connection the bolts are assumed to carry equal shear and a relatively free rotation occurs between the end of the beam and the supporting element. Shear tabs are considered as simple "Type 2" connections due to the rotation that occurs between the end of the beam and the supporting element. It achieves this rotation from: the bolt deformation in shear, the hole

distortion in the plate and/or the beam web, bolt slippage if the bolts are not in bearing at the time of initial loading, and the flexibility of the supporting element. However, due to the rigidity of the plate and the supporting element, the shear tab can develop moments in the end of the beam and the supporting member. This moment depends on: the number, size, and configuration of the bolt pattern; the thickness of the plate and/or the beam web; the beam span to depth ratio; the loading; and the relative flexibility of the supporting element.

Recent research [1] investigated the shear tab that was welded to a stiff supporting element such as an I-shaped column. This investigation consisted of: a series of single bolt shear tests for several bolt diameters and plate thicknesses; the generation of a finite element model to analyze the behavior of the shear tab connection; moment-rotation curves that were obtained through finite element modeling and small-scale testing; and a series of full-scale tests that were conducted to verify the adequacy of the analytical results. From this investigation, a procedure was recommended for the design and selection of shear-tab connections. The following steps, generalized from Reference 11, outline the procedure for the design of shear tabs that are welded to I-shaped columns as shown in Figure 1.1. This procedure is greatly simplified in the form of tables in Reference 11.

Step 1: Determine the length of the beam to the depth of the beam ratio.

l/d limitations:

noncomposite beams, F_y = 36 ksi: $l/d \leq 36$

noncomposite beams, F_y = 50 ksi: $l/d \leq 24$

Beams that exceed these limits should be checked for excessive end rotation.

Step 2: Determine the number of bolts required based upon the allowable bolt shear.

Step 3: $e(S)^{0.4} = h(e/h)_{ref} * n/N *(S_{ref})^{0.4}$, where

$(e/h)^{ref} = 0.06(l/d) - 0.15$ when $l/d \geq 6$

$= 0.035(l/d)$ when $l/d < 6$,

h = distance between center lines of top and bottom bolts in inches,

n = number of bolts,

N = 5 for 3/4-in. and 7/8-in. ϕ bolts

= 7 for 1-in. ϕ bolts, and

S_{ref} = 100 for 3/4-in. ϕ bolts

= 175 for 7/8-in. ϕ bolts

= 450 for 1-in. ϕ bolts.

Step 4: $e = [e(S)^{0.4}]/(S)^{0.4}$, where S in $(S)^{0.4}$ is the section modulus of the beam.

Step 5: $M = R(e + a)$; where

M = moment in the connection plate,

R = shear in the beam,

a = distance from the centerline of the bolt hole to the face of the column, and

e = as stated in Step 4.

Step 6: Size the A36 plate for stress and a minimum edge distance of 2 times the bolt diameter.

Step 7: Size the weld for combined shear and bending.

Step 8: Check to make sure the maximum plate thickness in the shear tab or the beam web is less than the following:

A325 3/4-in. ϕ bolts: $t \leq 3/8$ in.

7/8-in. ϕ bolts: $t \leq 7/16$ in.

1-in. ϕ bolts: $t \leq 9/16$ in.

A490 3/4-in. ϕ bolts: $t \leq 1/2$ in.

7/8-in. ϕ bolts: $t \leq 5/8$ in.

1-in. ϕ bolts: $t \leq 11/16$ in.

The procedure listed above is for beams that are uniformly loaded along the entire length. Eccentricity coefficients are listed in References 1 and 11 for several concentrated load configurations. As stated in the preceding paragraphs this design procedure is for shear tabs welded to stiff supporting elements. Appropriate factors of safety should be sought for flexible supporting elements[1,11].

2.3 Beam-line Theory

Beam lines are plots of end moment versus end rotation of a beam for a fixed load pattern and span. Beam lines are linear for constant magnitudes of load as shown in Figure 2.5. The vertical axis intercept in this figure is the fixed-end moment of the beam for the given load pattern and span while the horizontal axis intercept in this figure is the simple-span-end rotation of the beam. The intersection of a moment-rotation curve for a connection and the beam line results in the moment-rotation characteristic of the connection at the load increment in question. Generally, rigid "Type 1" connections carry approximately 90% or more of the fixed-end moment, whereas simple "Type 2" connections carry 20% or less of the fixed-end moment capacity. The region between these two curves is moment-rotation characteristics for the semi-rigid "Type 3" connection[4].

Beam-line plots can be useful in the design of connections if their moment-rotation characteristics are known. The strength, M_i, of the connection can be designed so that the end rotation, θ_i, of the joint is compatible with the rotation that results from a particular load pattern.

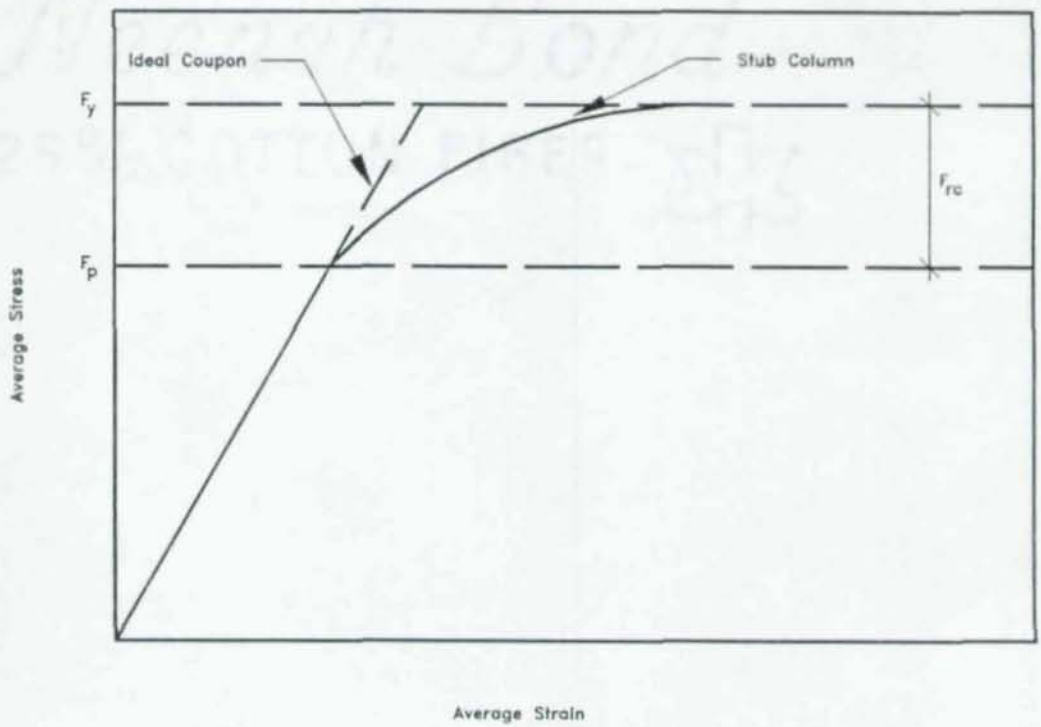

Figure 2.1: Generalized Stress–Strain Relationship

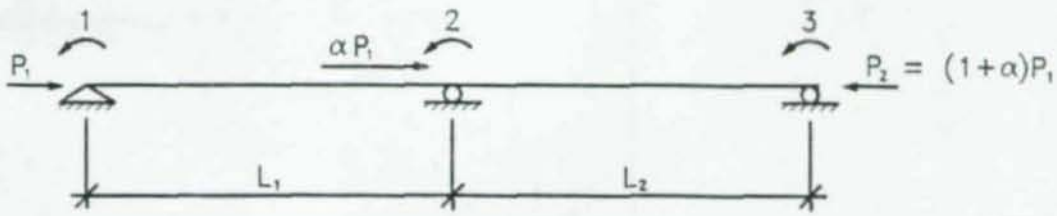

$$S_G = \begin{bmatrix} S_{FF} & S_{FR} \\ S_{RF} & S_{RR} \end{bmatrix}$$

$$S_G = EI \begin{bmatrix} C_3 & C_4 & 0 & C_2 & -C_2 & 0 \\ C_4 & C_3+C_7 & C_8 & C_2 & -C_2+C_6 & -C_6 \\ 0 & C_8 & C_7 & 0 & C_6 & -C_6 \\ C_2 & C_2 & 0 & C_1 & -C_1 & 0 \\ -C_2 & -C_2+C_6 & C_6 & -C_1 & C_1+C_5 & -C_5 \\ 0 & -C_6 & -C_6 & 0 & -C_5 & C_5 \end{bmatrix}$$

$$S_{FF} = EI \begin{bmatrix} C_3 & C_4 & 0 \\ C_4 & C_3+C_7 & C_8 \\ 0 & C_8 & C_7 \end{bmatrix}$$

Where:

$C_1=12S_{11}/L_1^3$, $C_2=6S_{21}/L_1^2$, $C_3=4S_{31}/L_1$, $C_4=2S_{41}/L_1$,

$C_5=12S_{12}/L_2^3$, $C_6=6S_{22}/L_2^2$, $C_7=4S_{32}/L_2$, $C_8=2S_{42}/L_2$,

$S_{11}=[T_1^3\sin(T_1)]/12\phi_c$, $S_{21}=[T_1^2(1-\cos(T_1)]/6\phi_c$,

$S_{31}=[T_1(\sin(T_1)-T_1\cos(T_1)]/4\phi_c$, $S_{41}=[T_1(T_1-\sin(T_1)]/2\phi_c$,

$\phi_c=2-2\cos(T_1)-T_1\sin(T_1)$, $T_1=(L_1)(P_1/EI)^{0.5}$, $T_2=T_1\ [1+\alpha]^{0.5}$, and

$K_1 = \pi/T_1$.

Figure 2.2: Effective Length Determination

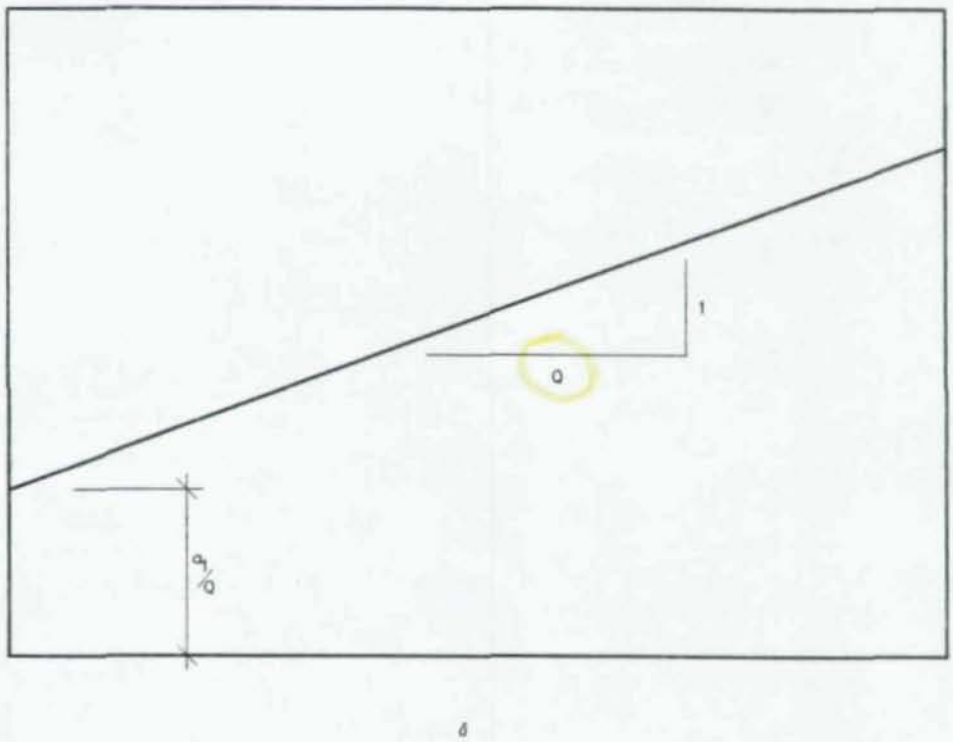

Figure 2.3: Southwell Plot of Central Displacements

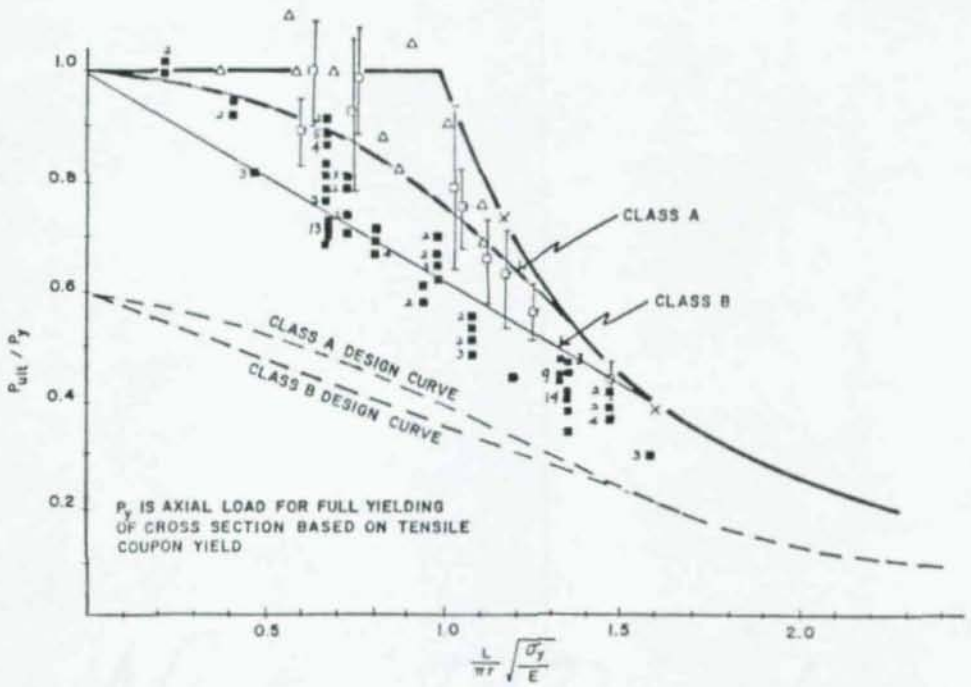

Figure 2.4: Test Data for Axially Loaded Rectangular Tubes

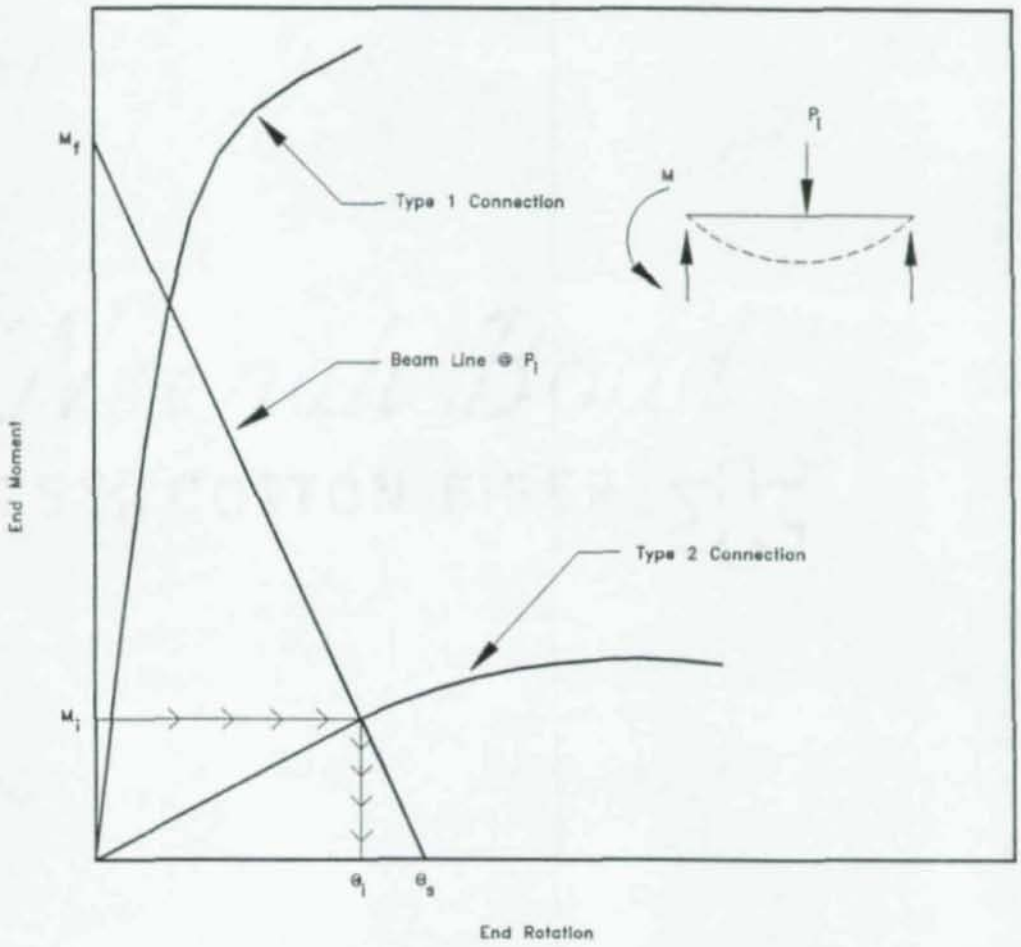

Figure 2.5: Beam Line at Service Load

3. TEST PROGRAM

3.1 Test Description

In this investigation four column tests were conducted to evaluate the behavior of rectangular-tubular columns with shear tabs welded to their walls as shown in Figure 3.1. The test specimens of this investigation were subdivided into two groups: the control group and the test group. The control-group specimens consisted of two rectangular tubes with through plates welded at mid-height. This type of connection is often specified in place of the shear tab in order to reinforce the tube wall. The test-group specimens consisted of two rectangular tubes with shear tabs welded at mid-height. Figure 3.2 shows the two connections used in this investigation.

In one pair of specimens, a control column and a test column, the bolts were snug tightened while in the other pair, they were fully tightened as in a slip control connection. Snug-tight bolts were used in one pair of specimens to determine if this new method of bolt tightening would affect the column capacity in comparison with fully-tightened bolts. The concern is that with limited rotational restraint (hinges) at the face of the tube and at the bolt line, a mechanism could form that would greatly increase the wall distortion.

3.2 Test Design

3.2.1 Column Selection

At the University of Wisconsin-Milwaukee's structural testing facility, the maximum compressive load that can be applied to long columns is approximately 200 kips. The maximum length that the column can be is approximately 26 feet. As a result, a 20-foot column length was selected to achieve story heights of 10 feet. Due to the availability and the small number of specimens needed, a 6 X 3 X 5/16 inch rectangular tube with a nominal yield strength of 46 ksi was selected for the column specimens.

3.2.2 Beam Selection

Generally, in building design, beams are designed for uniformly applied loads or for multiple concentrated loads. However, uniform or multiple concentrated loads are difficult to apply to the test beam because they would require additional loading mechanisms that are not available. With this in mind, a single concentrated load was placed at a point on the beam to achieve the reaction and the end rotation that would result from a uniformly loaded beam of the same length for a load of 125 pounds per square foot (See Figure 3.3). As a result, a concentrated load of 40 kips at a distance of 4.5 feet from the centerline of the column (12.5 feet from the far end of the beam) was used to design the beams. The selection of this load pattern was based on the available locations that the

concentrated load could be applied to the beams by the loading system. From this load pattern, a W12 X 53 section of A36 steel was selected for the framing beams due to the availability of materials in the Milwaukee area.

3.2.3 Connection Selection

The shear tabs used in this investigation were designed in accordance with the procedures and recommendations of References 1 and 11 with the assumption that the eccentricity in the connection occurs at the bolt line due to the flexibility of the tube wall. The connections were designed for a vertical reaction of approximately 40 kips. However, the connections were only loaded to a vertical reaction of 30 kips during each test. Three standard A325-X bolts of 3/4-inch diameter were required to resist the 40-kip reaction. From the provisions in Reference 1 and the above information, a 9 X 4.5 X 5/16 inch plate was used as the shear tabs as shown in Figure 3.4. The through plates were identical to the shear tabs except that they were continuous over the 12 inch length.

The procedure that was used from Reference 1 was developed for shear tabs connected to the flanges of I-shaped columns. However, this design method with modified eccentricity was used because it is the only one that was available. The connection design for the shear tabs incurred in this investigation is provided in Appendix A.

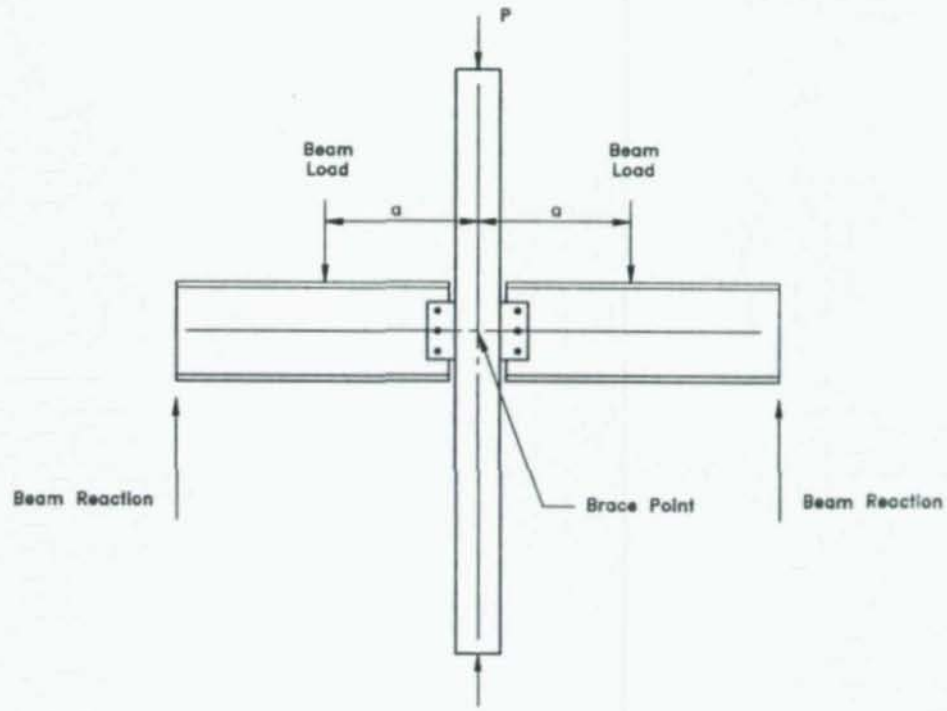

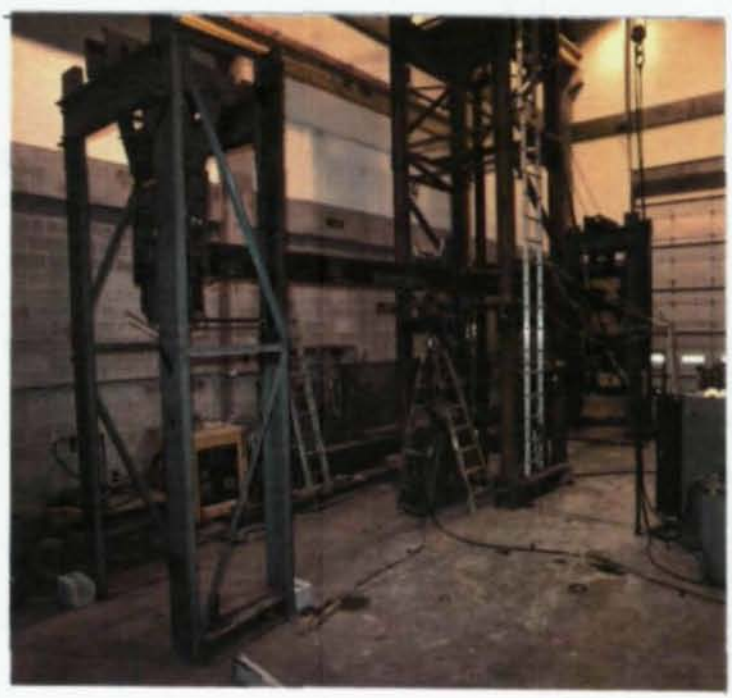

Figure 3.1: Test Setup

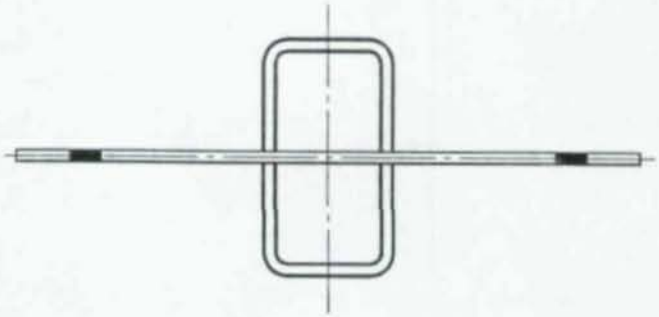

A. Through-Plate Connection

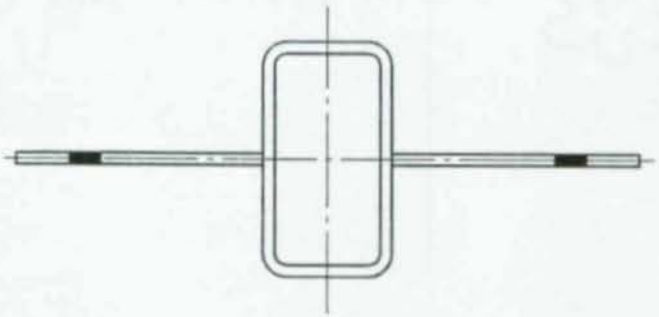

B. Shear Tab Connection

Figure 3.2: Connection Types

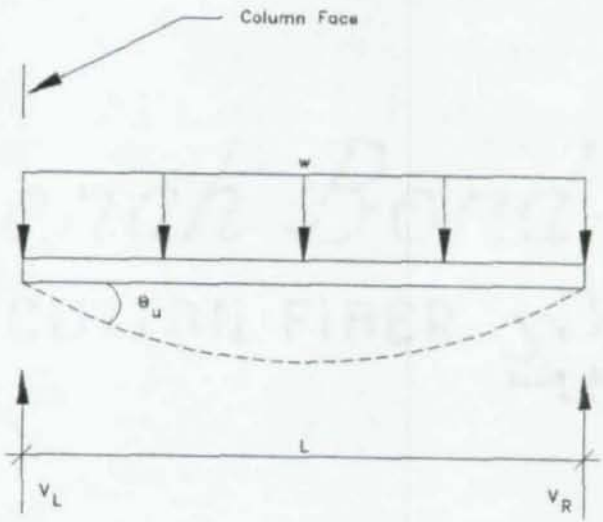

$$V_L' = V_L$$

$$\frac{Pb}{L} = \frac{WL}{2}$$

$$Pb = \frac{WL^2}{2}$$

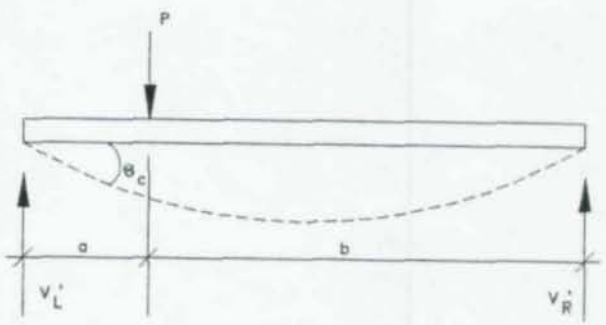

$$\theta_c = \theta_u$$

$$\frac{Pb\,(L^2 - b^2)}{6LEI} = \frac{WL^3}{24EI}$$

$$Pb\,(L^2 - b^2) = \frac{WL^4}{4}$$

Figure 3.3: Beam Load Location

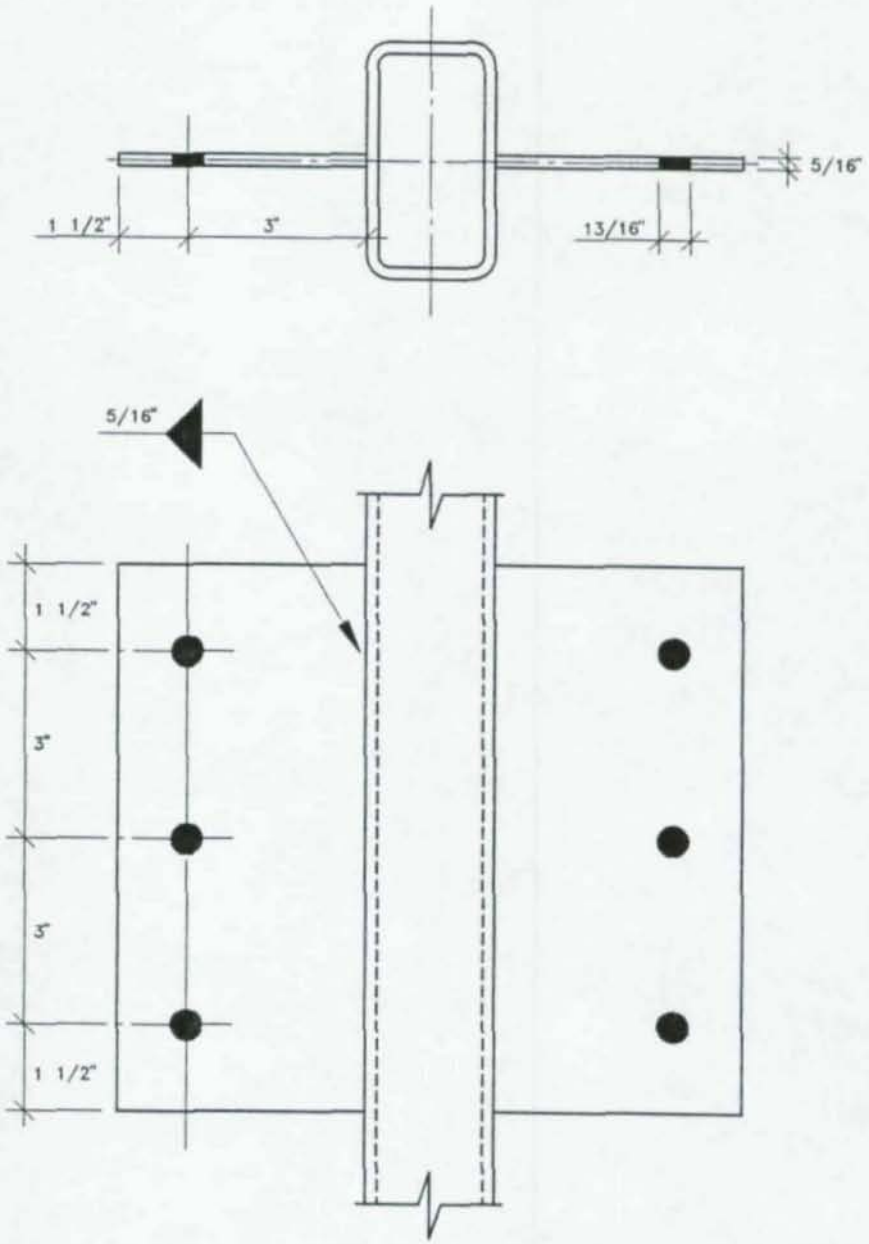

Figure 3.4: Test Shear Tab Connection

4. TEST PROCEDURE

4.1 Loading System

Figures 4.1 to 4.4 illustrate the components of the loading system that were used in this investigation. The loads applied to the system are shown in Figure 4.1.

The axial load that was applied to the top of the tubular columns was produced by two hydraulic jacks. These jacks were centered upside down in a 30-foot loading tower, thereby producing two compressive concentrated loads as shown in Figure 4.2. These concentrated loads were applied to the column through a hinged plate that was welded to the top of the column while a similar hinged plate was welded to the bottom. These plates allow the ends of the column to rotate thereby functioning as pinned ends.

The concentrated loads that were applied to the framing beams were produced by a threaded rod that passed through the ram of a hydraulic jack that was mounted in a Gravity Load Simulator (GLS). The GLS is a mechanism that remains stable only under a tensile load that is produced in the rod with the rod passing through the intersection of the lines of action of the two side tension bars. As a result, vertical alignment of the loading rod is maintained at all times. The other end of the loading rod was attached to a hinged-plate assembly which bears directly on the framing beam at the point of loading while maintaining vertical alignment. These fixtures were previously used in Reference

12 and converted to meet the needs of this investigation as shown in Figure 4.3.

The reactions at the far ends of the framing beams were obtained by using two more gravity load simulators and hinged-plate assembly systems. However, this reaction system was mounted upside down in a 16-foot tower that was anchored to the floor as shown in Figure 4.4. Again a loading rod was used to connect the GLS to the hinged-plate assembly. The end of beams rested on the hinged plate of this assembly. To produce a braced frame, a cable and turnbuckle system was used to provide an axial brace in these beams to prevent the column from lateral movement at the connection.

4.2 Instrumentation

As stated previously, there were two types of tests conducted for each specimen: a connection test and a column test. For these tests several items of instrumentation were used to measure loads, displacements, strains, and rotations as shown in Figure 4.5. Each piece of instrumentation was calibrated prior to test setup or each test run.

For both tests, the loads on the floorbeams as well as the beam reactions were measured by strain-gaged loading rods. These rods were used to attach the GLS to the hinged-plate assembly as described in the previous section. The axial loads that were applied to the top of the column were measured by two strain-gaged load cells that were attached

to the hydraulic rams positioned in the 30-foot loading tower.

Lateral deflections were measured at three locations along the length of the column during each test; at the middle of each segment and at the connection. These deflection were achieved by placing linear-voltage-displacement transducers (LVDT) at the three locations as shown in Figure 4.5. LVDT's produce a voltage change for a given change in movement which is then converted to a displacement in a data acquisition system.

In the testing of the connection, two linear strain gages were mounted approximately 8.75 inches apart on each connecting plate top and bottom edges near the tube wall. These gages were used to validate the moment that was produced in the connection near the face of the column. Furthermore, a Tee-strain gage was mounted approximately one inch below the connection plate on each side of the column. These strain gages were used to compare the effects that the two types of connections had on the load transfer mechanism and on column behavior.

Rotations were measured at the bolt line of the beam-column connection to check the flexibility of the connection. These rotational measurements were made by a pendulum device that produced a calibrated motion in a LVDT. These so called "slope indicators" are very sensitive to motion and may not be reliable for small rotations.

However, they were used to roughly verify the rotations calculated by beam-line theory.

4.3 Data Acquisition

With all of this instrumentation being used, a data acquisition system was highly desirable. All of the instrumentation was connected to a 32 Channel Kaye III Digistrip Datalogger by way of transducer conditioner boxes. A printout of the instrumentation parameters was obtained during each test.

In addition to the datalogger, a personal computer was used to store the test data on a floppy disk. The values stored on this disk were voltages obtained from the conditioner boxes and the instrumentation. With the aid of spread sheet software, these values were converted to loads, strains, displacements, and rotations knowing the calibration numbers of the instrumentation.

4.4 Test Procedure

The following identification system was used in order to distinguish among the connection configurations for the tests:

1. PT = the through plate connection with tight bolts.
2. TT = the shear tab connection with tight bolts.
3. PS = the through plate connection with snug-tight bolts.

4. TS = the shear tab connection with snug-tight bolts.

The identification system shown above is also listed in the order in which the specimens were tested.

4.4.1 Connection Test

After zero readings were recorded, axial load was applied to the column until a 10-kip reading was obtained, 5 kips in each load cell. The 10-kip load was used to stabilize the frame system. While the 10-kip reading was maintained, the North beam was loaded to 5, 10, and 20 kips. While the 20-kip North beam load and the 10-kip column load were maintained, the South beam was loaded in the same manner as the North beam until a balanced load condition was achieved. After the balanced load condition was achieved, the North beam load was unloaded to 10 kips and to zero load while maintaining the 20-kip South beam load and the 10-kip column load. Next the South beam load was unloaded to zero in the same manner. Finally, the column load was brought to zero load. Loads, displacements, strains, and rotations were recorded after each load increment. Zero load readings were taken again to see if all the readings returned to zero.

The connection tests were conducted in order to achieve the behavior of these connections under service loads. It is not the intent of this investigation to load the

connections to failure. Therefore, the connection tests are incomplete.

4.4.2 Column Test

After the zero readings were recorded, load was applied to the column until a 10-kip reading was obtained as in the connection test stated above. While this column load was maintained, both beams were loaded simultaneously in increments of 10 kips until the maximum designed load of 40 kips was obtained. While the beam loads were maintained at 40 kips, more column load was applied in 20-kip increments. This loading increment was adhered to until near failure was reached. After severe buckling and loss of load occurred the test was terminated.

4.5 Material Properties

4.5.1 Tension Tests

In order to obtain the yield strength of the material one tensile coupon was cut from the upper end of two of the tubular columns and milled down to the specifications of the ASTM A370.

These tensile coupons were tested at a slow rate in a tension testing machine that plotted a graph that contained the load versus strain for the particular specimen.

4.5.2 Stub Column Test

A stub column test was conducted to determine the average compressive strength of the cross section. The stub column consisted of a 20-in. long section that was cut from the top of one of the test columns that were not used for the tensile coupons. This stub column was prepared according to the recommendations outlined in Reference 2.

In order to obtain a stress-strain curve of the cross section, Tee-strain gages were mounted on each side of the stub column at its mid-height. From these readings and the load obtained from the testing machine a load versus strain plot was constructed. With this in mind, one of the strain gages and the load from the testing machine were connected to an X-Y plotter to monitor the progress of the test.

After zero readings were recorded in the automatic data logger, the stub column was loaded in increments of 20 kips until the proportional limit was clearly defined on the curve produced by the X-Y plotter. After the proportional limit was achieved the column was then loaded in increments of 10 kips until the test was terminated. The test was terminated after a load of 330 kips was achieved since the axial load was hard to stabilize on the testing machine. However, the test was long enough to achieve enough data points in the plastic range to determine the yield strength of the material.

4.6 Data Reduction

During each test several items of data were recorded by the data acquisition system. For this investigation a personal computer was utilized for the purpose of automatic data acquisition onto a floppy disk. The information on this disk is the loads, strains, displacements, and rotations that are recorded by the datalogger for each load increment. Along with computer software, this information was converted to the final form that is listed in the test results. The rest of this section presents the equations that were used to achieve the desired results of this investigation.

4.6.1 Eccentricity Analysis

The eccentricity in the connection can be generalized as the moment in the connection divided by the shear at the end of the beam. The moment in the connection at the tube wall is as follows:

$$M_{conn} = .5(\epsilon_t - \epsilon_b)S_{pl}E$$
$$= .0612(\epsilon_t - \epsilon_b) \qquad (4.1)$$

where M_{conn} = connection moment, in.-kip

ϵ_t = strain in top of plate, μin./in.

ϵ_b = strain in bottom of plate, μin./in.

S_{pl} = section modulus of plate, 4.22 $in.^3$

E = 29000 ksi

Now the eccentricity in the connection is

$$e_{conn} = M_{conn}/V_{beam} - 2.375 \qquad (4.2)$$

where $V_{beam} = P_{beam} - R_{beam}$,

R_{beam} = beam reaction

The constant of 2.375 subtracted in Eqn. 4.2 is the average distance from the center of the bolt line to the center of the linear strain gages. Therefore, the eccentricity is measured with respect to the bolt line.

4.6.2 Beam-Line Analysis

The information required for the construction of a beam-line plot are: the fixed-end moment for each load increment; the simple-span-end rotation for each load increment; and the experimental moment in the connection. The fixed-end moment in the beam is

$$M_i = P_i(a)[L^2 - a^2]/2L^2$$

$$= 33.85\ P_i \text{ (in-kips)} \qquad (4.3)$$

and the simple-span rotation is

$$\theta_i = P_i(a)[L^2 - a^2]/6LEI$$

$$= .000185\ P_i \text{ (radians)} \qquad (4.4)$$

where P_i = beam load

a = 150 in.

L = beam length to face of tube, 202.5 in.

E = 29000 ksi

I = moment of inertia, 425 $in.^4$

Refer to Eqn. 4.1 for the experimental moment in the connection.

4.6.3 Elastic Stresses in the Tube Wall

The elastic stresses in the tube wall were computed using the equation of biaxial stress in terms of strains. The stresses are:

$$F_{long} = E^*(\epsilon_{long} + \nu\epsilon_{tran})/(1 - \nu^2)$$

$$= 31868\ [\epsilon_{long} + 0.3\epsilon_{tran}] \qquad (4.5)$$

$$F_{tran} = E^*(\epsilon_{tran} + \nu\epsilon_{long})/(1 - \nu^2)$$

$$= 31868\ [\epsilon_{tran} + 0.3\epsilon_{long}] \qquad (4.6)$$

where F_{long} = longitudinal stress, ksi

F_{tran} = transverse stress, ksi

ϵ_{long} = longitudinal strain, in./in.

ϵ_{tran} = transverse strain, in./in.

$E = 29000$ ksi

$\nu = 0.3$

The strains, longitudinal and transverse, are recorded in the tables of Appendix E for each of the four tests.

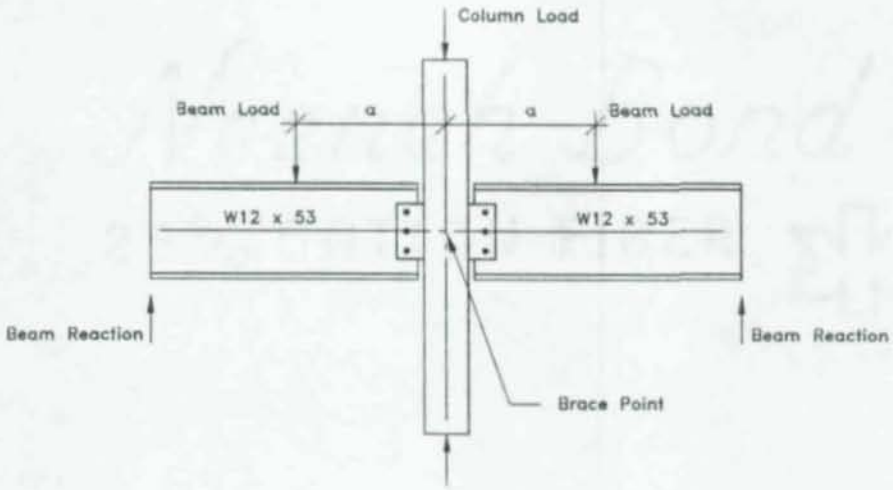

Figure 4.1: Schematic of Loading

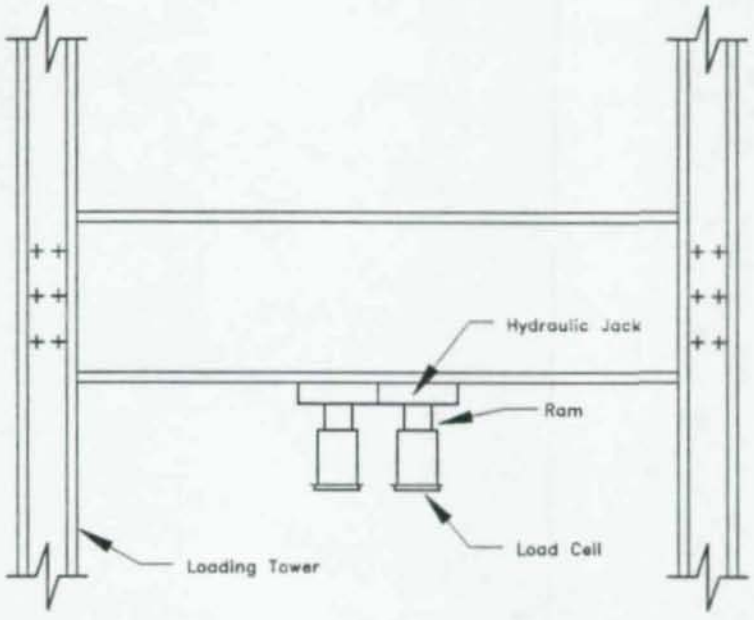

Figure 4.2: Column Loading Mechanism

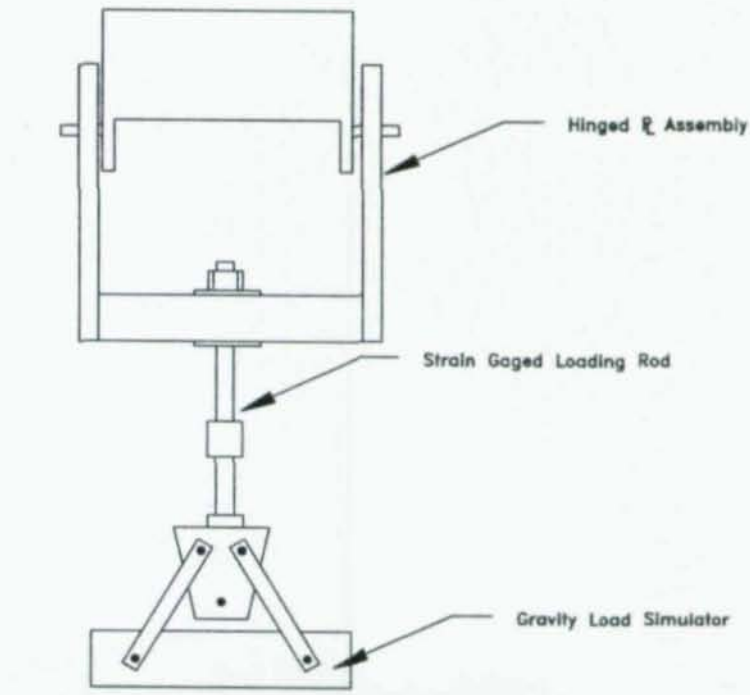

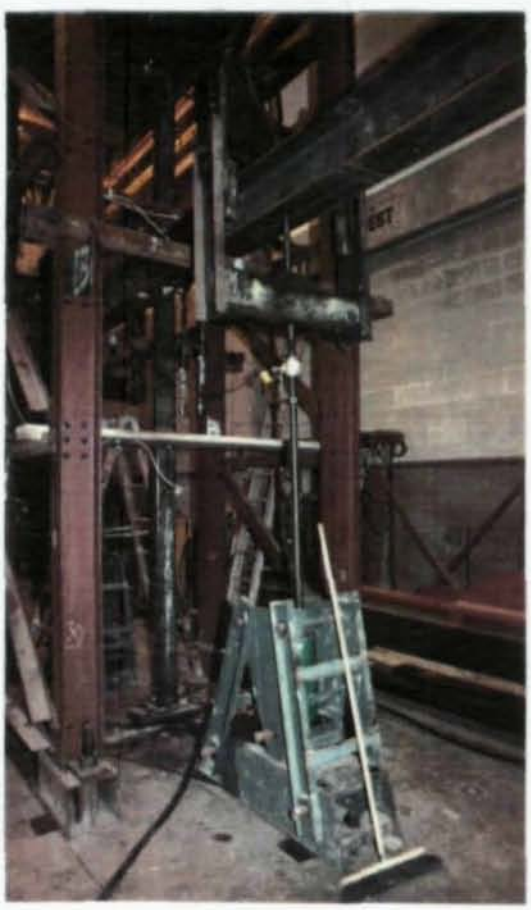

Figure 4.3: Beam Load Mechanism

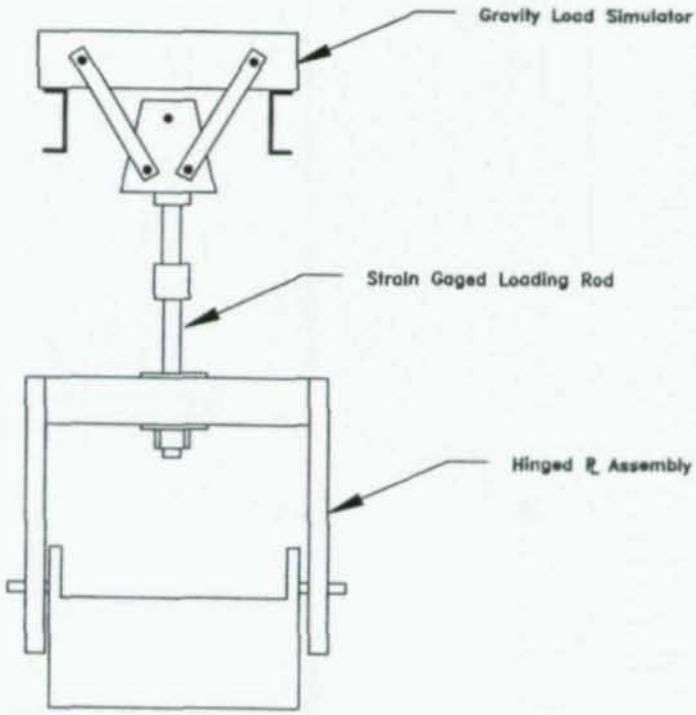

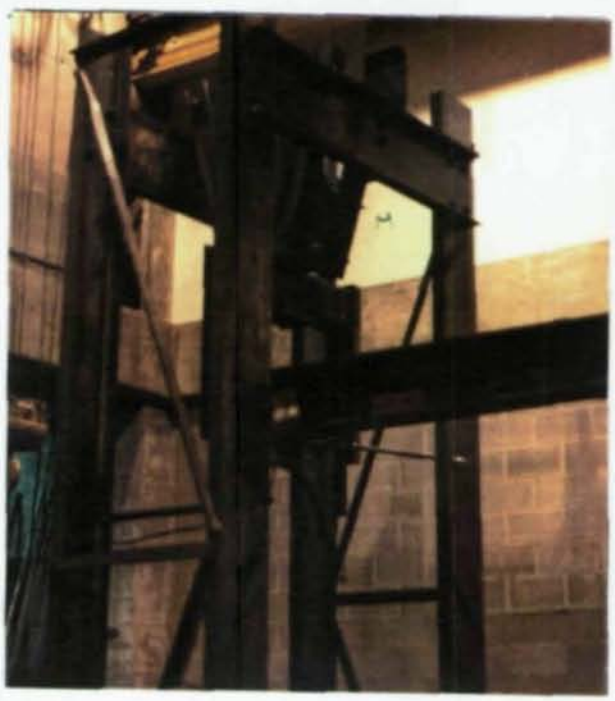

Figure 4.4: Beam Reaction Mechanism

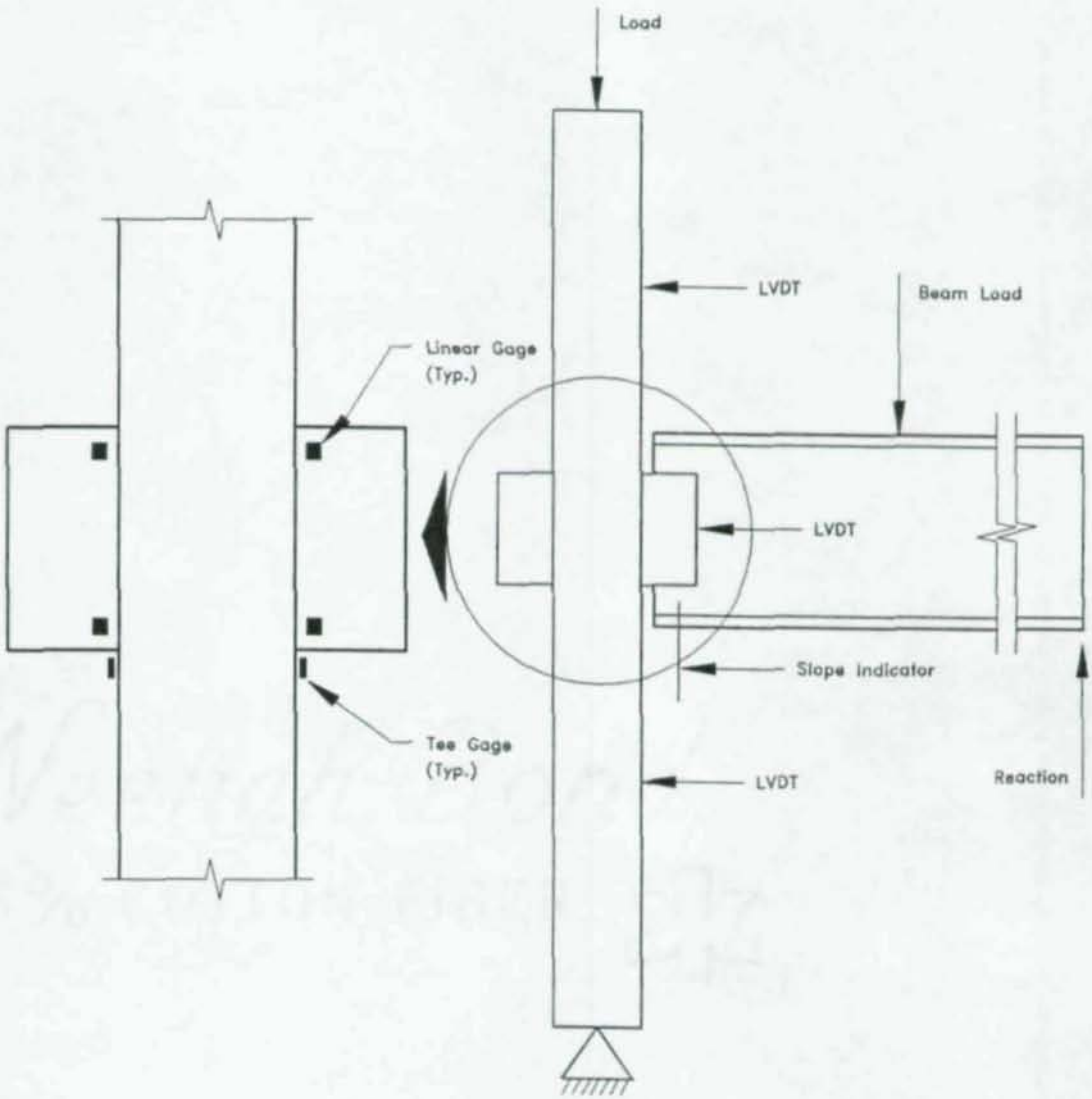

Figure 4.5: Instrumentation Schematic

5. GENERAL TEST RESULTS

5.1 Individual Test Results

The detailed results of each of the four tests are contained in Appendix E of this paper. The following information is provided for each of the individual tests:

1. Data tables consisting of loads, displacements, and strains obtained during each connection test and each column test.
2. Plots of load versus lateral displacement of the lower column.
3. A plot and photo of the buckled shape.

Some of the information presented in Appendix E was not used directly in the evaluation of the column or connection behavior. However, it has been retained to provide additional information for any secondary factors affecting the test results.

5.2. Material Properties

Figure 5.1 contains the stress-strain curves for the two tension tests that were conducted to determine the yield strength of the material. Using the 0.2 percent offset method, the yield strengths for the two tensile coupons are 65 and 71 ksi. However, the mill test report that accompanied the test specimens indicates that the yield strength of the material is 57.3 ksi, well below that obtained from the tension tests. For this reason, a stub

column test was conducted to obtain an average yield strength over the entire cross-section.

The stress-strain curve for the stub column test is shown in Figure 5.2. Again, using the 0.2 percent offset method, the average yield strength of the cross section is approximately 65 ksi. The strain information that was used in this curve was obtained from four strain gages that were mounted on the 20-inch long stub column at its midheight. The strain readings plotted are an average of the four readings.

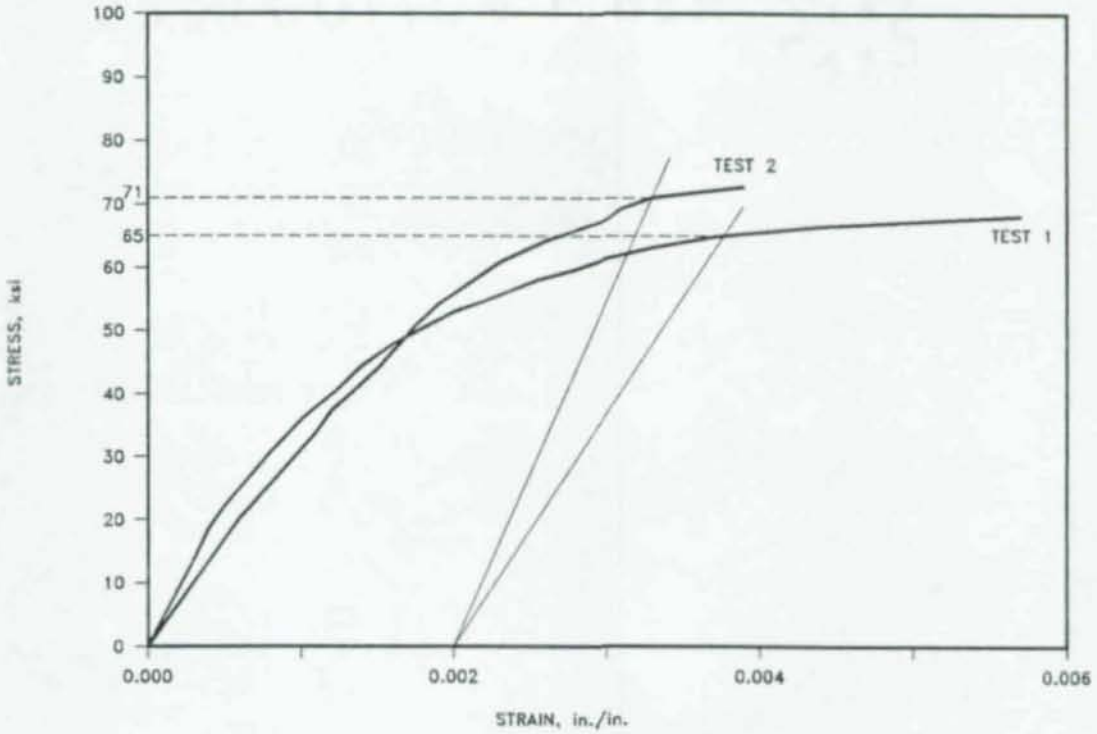

Figure 5.1: Tension Test Curves

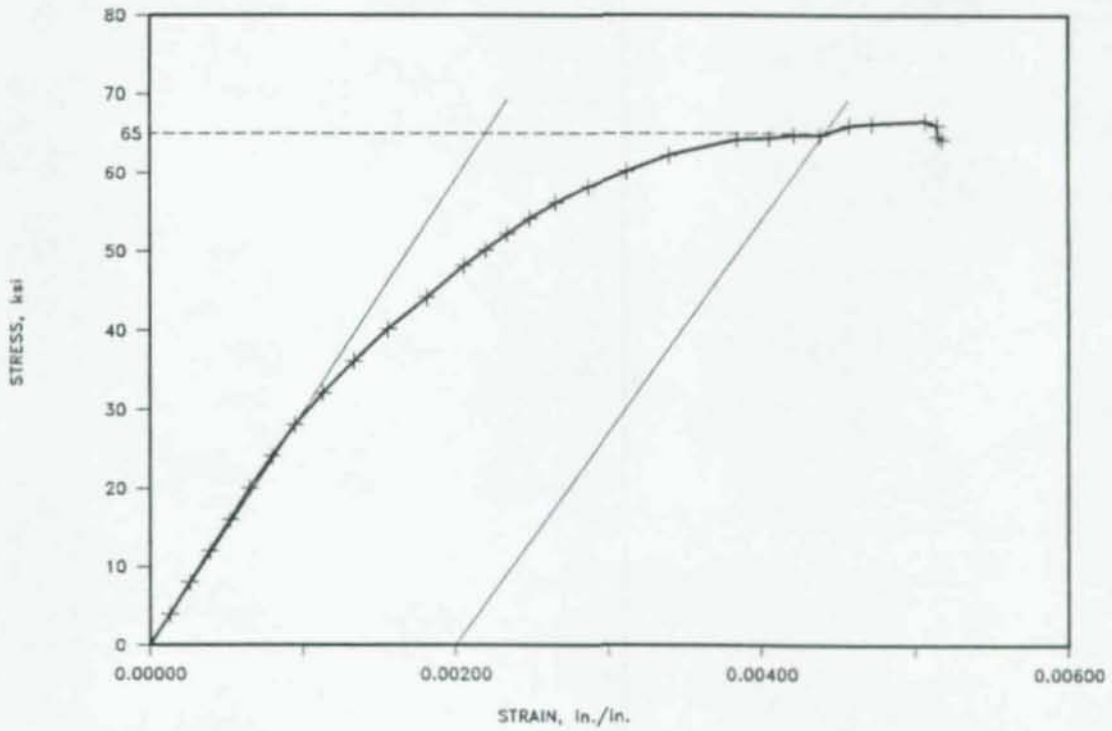

Figure 5.2: Stub Column Curve

6. CONNECTION BEHAVIOR

6.1 Experimental Results

Figures 6.1 and 6.2 are plots of beam load versus load eccentricity in the connection. Figure 6.1 contains the plots for each of the four tests for an unbalanced load condition. The unbalanced load condition is the loading sequence where one beam was loaded while the other beam was held at zero load during the connection test. The straight plateaus at the 20-kip load represent the loading of the South beam until a balanced load condition was reached. In addition, Figure 6.2 represents the plots of beam load versus load eccentricity in the connection for each of the four tests under a balanced load condition. The balanced load condition is the loading sequence where both beams were loaded simultaneously until the 40-kip load was reached during the column test.

In addition to the beam load versus eccentricity plots, Table 6.1 is a list of the load eccentricities for each test for a 30-kip reaction under a balanced load condition. Also listed in this table is the theoretical load eccentricity for the shear tab connected to a very stiff supporting element. The theoretical eccentricity was determined using the procedure that is outlined in Section 2.2 of this paper. The eccentricities listed in Table 6.1 are measured with respect to the bolt line.

Figures 6.3 and 6.4 are beam-line plots for the tests and data under concentrated loads of 0 to 40 kips. For clarity the data for PT and TS specimens were only plotted in Figure 6.3. However, Figure 6.4 is a beam-line plot containing data points for the four tests with the vertical axis enlarged.

The stresses in the tube wall are shown in Figure 6.5 for a balanced 30-kip reaction for each of the four tests. The elastic stresses were obtained from the T-strain gages that were mounted one-inch below the connection plates. The longitudinal and transverse stresses shown in Figure 6.5 were computed using the equation of biaxial stress in terms of strain and Hooke's law assuming an elastic modulus of 29000 ksi and a poisson's ratio of 0.3.

Figures 6.6 to 6.9 are plots of beam load versus strain in the tube wall, one-inch below the connection plates, for each of the four tests. Figures 6.6 and 6.7 are beam load versus longitudinal strain plots for unbalanced and balanced load conditions, respectively. Figures 6.8 and 6.9 are beam load versus transverse strain plots for unbalanced and balanced load conditions, respectively. The data for the unbalanced load condition was obtained from the connection tests while the data for the balanced load condition was obtained from the column tests. The data used in these plots are taken directly from the tables listed in Appendix E for each of the four tests.

6.2 Discussion of Results

The experimental load eccentricities in the end of the beam under a reaction of 30 kips range from 1.13 inches to 4.08 inches from the bolt line as shown in Table 6.1. However, the theoretical load eccentricity is 3.83 inches from the bolt line according to the procedure outlined in Section 2.2 of this paper. For the most part, the experimental load eccentricities are less than the theoretical value. The variation in these eccentricities is primarily due to the difference in flexibility of the supporting elements for the tests specimens and the design procedure.

The calculation of the theoretical load eccentricity is based on the research of shear tabs that are welded to stiff supporting elements[1]. The shear tabs in this research are welded to the flange of an I-shaped column in line with the web. However, the joint configuration for the shear tabs in this investigation have connection plates welded to the walls of the tubular column. Since the shear tabs are welded in the middle of the tube wall a rotational distortion occurs when the connection is loaded. This rotation results in a smaller load eccentricity in the connection depending on the relative stiffness of the tube wall. Therefore, the experimental load eccentricity is smaller than the theoretical load eccentricity.

The experimental eccentricities for the through plate connection would be expected to be somewhat closer to the

theoretical eccentricity. However, three of the four experimental load eccentricities for the PT and PS specimens are still less than the theoretical load eccentricity (See Table 6.1). If the depth of the through plate were substantially larger, the experimental eccentricities would be expected to approach the theoretical values.

The beam load versus eccentricity plots for the unbalanced load condition, Figure 6.1, indicate that the loading sequence greatly affects the eccentricity in the connection. This is evident by the difference between load eccentricities for each side of the column at the 20-kip load in Figure 6.1.

The investigation of the shear tab connected to a stiff supporting element [1] verified that the shear tab connection functions as a simple "Type 2" connection. As one might expect, the shear tab welded to rectangular-tubular columns, as they are in this investigation, also functioned in the range considered as simple "Type 2" connections as shown in Figures 6.3 and 6.4. However, the rotation that occurs from a particular load increment cannot exceed the end rotation of an ideally simply supported beam for the same load pattern and span. The maximum end rotation in the beam with a 30-kip reaction is 0.0074 radians (shown as the horizontal axis intercept in Figures 6.3 and 6.4). More important, the local distortion in the tube wall that is generated by a simply supported beam

cannot exceed this rotation. Therefore, the rotation in the connection can be considered as self-limiting.

The elastic stresses in the tube wall under a beam reaction of 30 kips, shown in Figure 6.5, indicate that there is a difference in the way the loads are transferred to the column. For instance, the longitudinal stresses in the tube wall for the TT and TS specimens are more than twice those of the PT and PS specimens. More important is the dramatic increase in transverse stress in the tube wall for the TT and TS specimens as compared to the PT and PS specimens. This variation is primarily due to the difference in load transfer mechanisms for the two types of connecting elements.

The load transfer mechanism for the through plate is quite simple. The shear in the connection is resisted by the tube wall through the welds along the sides of the connecting plate. The moment in the connection that results from the eccentric load in the beam is resisted by both the tube wall and the through plate. The majority of the moment in the connection, under a balanced load condition, is resisted by the through plate which is evident by the small transverse stresses in the PT and TT specimens in Figure 6.5. However, the amount of moment that is resisted by the through plate and the tube wall is indeterminate.

The load transfer mechanism for the shear tab is similar to that of the through plate except that all of the loads in the connection are resisted by the tube wall. The

shear in the connection is resisted by tube wall as stated above for the through plate connection. However, the applied moment is resisted solely by the tube wall. This would account for the very large increase in transverse stress for the shear tabs in comparison with the through plates.

In short, the primary difference between the shear tab connection and the through plate connection is their load transfer mechanisms. The load eccentricity, the tube wall stresses, the end rotation, and the strains are all dependent on the load transfer mechanisms of the two connections.

The variables that affect the behavior of the shear tab welded to rectangular-tubular columns are the flat width to thickness ratio, w/t, and the stiffness of the framing beams. The w/t ratio of the longest side of the tubular columns used in this investigation is 19. A rectangular-tubular column with a smaller w/t ratio would tend to have a stiffer tube wall which would resist more rotational distortion than the columns of this investigation. As a result, the end rotation will decrease while the load eccentricity will increase. On the other hand, the wall of a tubular column with a larger w/t ratio will become more flexible than the test specimens in this investigation. The local distortion of the tube wall for this situation will be somewhat greater than in this investigation, but still limited. Since the tube wall is more flexible, the end

rotation will increase and the load eccentricity in the connection will decrease.

The other variable that affects the behavior of the shear tab connection is the flexural stiffness of the framing beam. Increasing the beam stiffness from that of the test beams, but having the same column section, will result in a decrease the end rotation of the beam and in load eccentricity in the connection. Similarly, the end rotation and the load eccentricity will increase for a reduction in the beam stiffness.

The magnitudes of the changes in the load eccentricity and the end rotation for various beam sizes and column sizes requires further investigation.

Specimen	E_{north}	E_{south}	E_{theor}
PT	1.37"	4.08"	
TT	1.49"	1.13"	
PS	1.51"	2.99"	
TS	1.54"	2.66"	
Ave	1.48"	2.71"	3.83"

Table 6.1: Connection Eccentricities at 30 kip Reaction

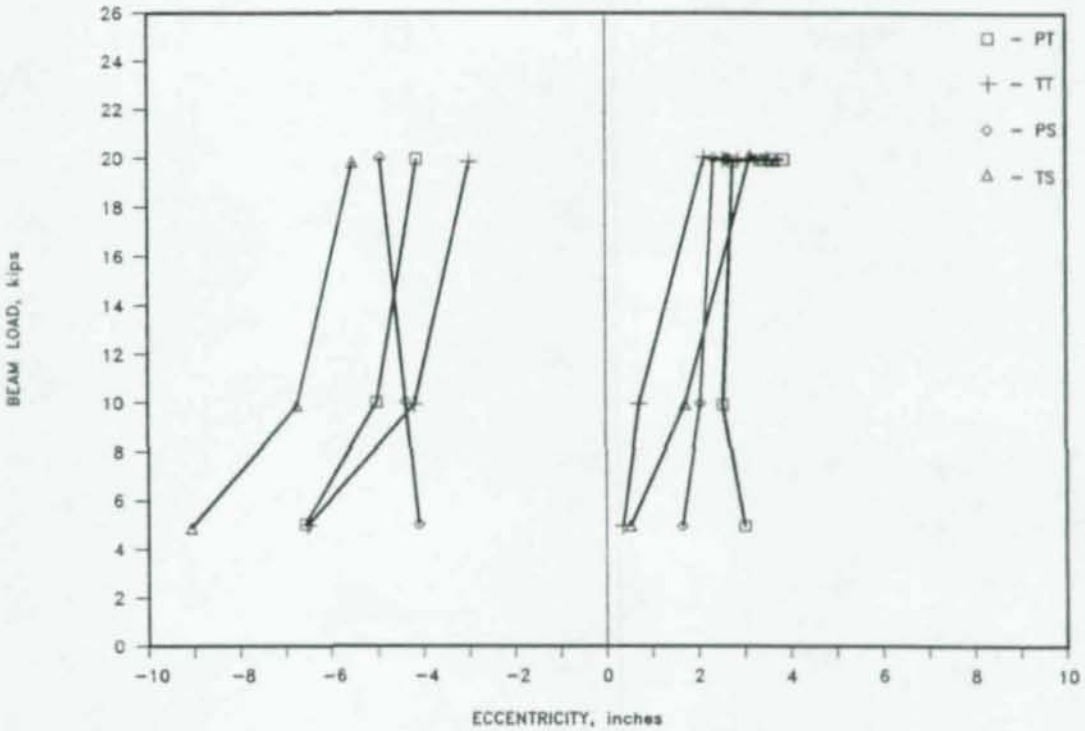

Figure 6.1: P_{beam} vs. E_{conn} – Unbalanced Load Condition

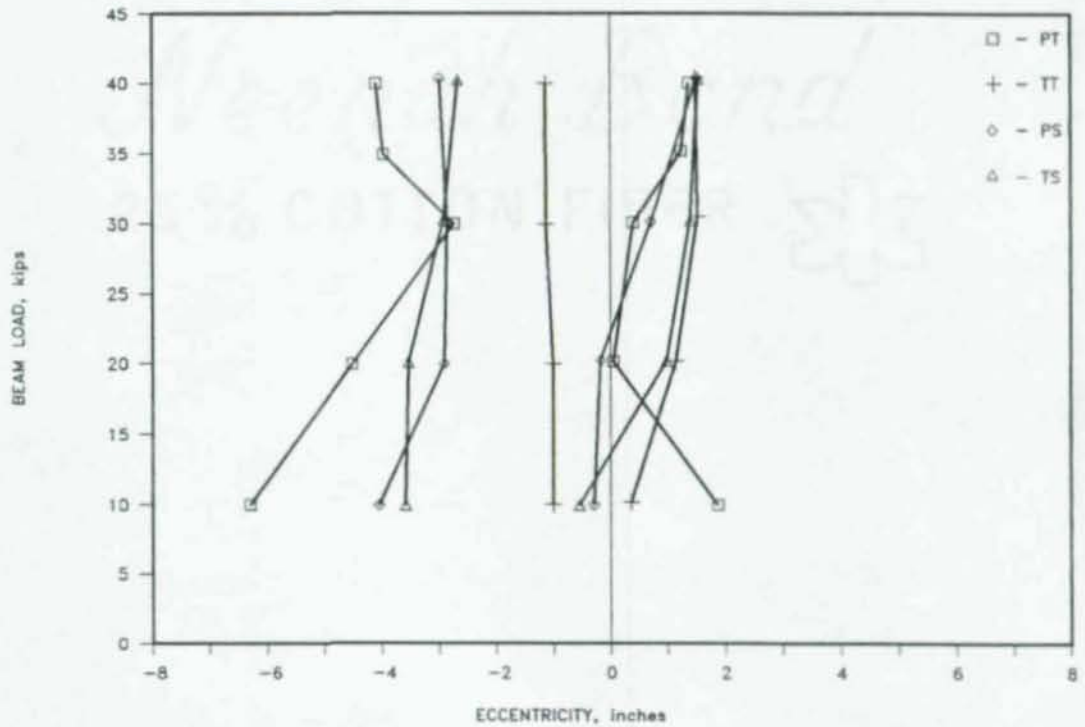

Figure 6.2: P_{beam} vs. E_{conn} – Balanced Load Condition

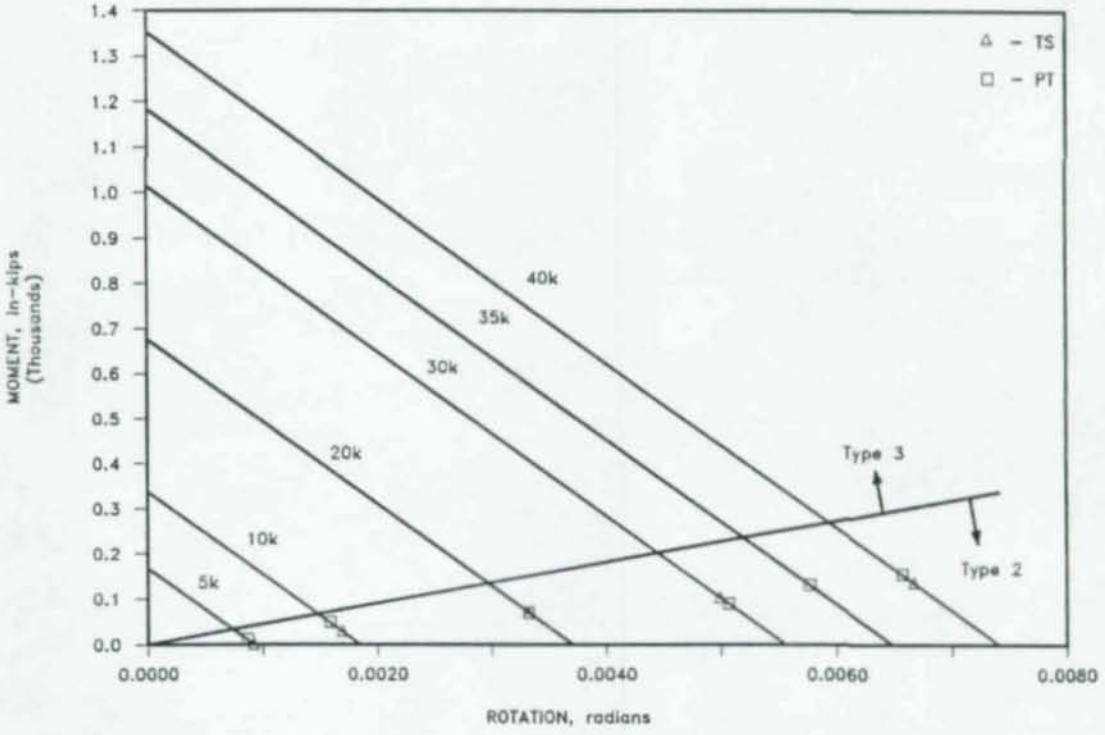

Figure 6.3: Beam-Line Plot PT & TS Specimens

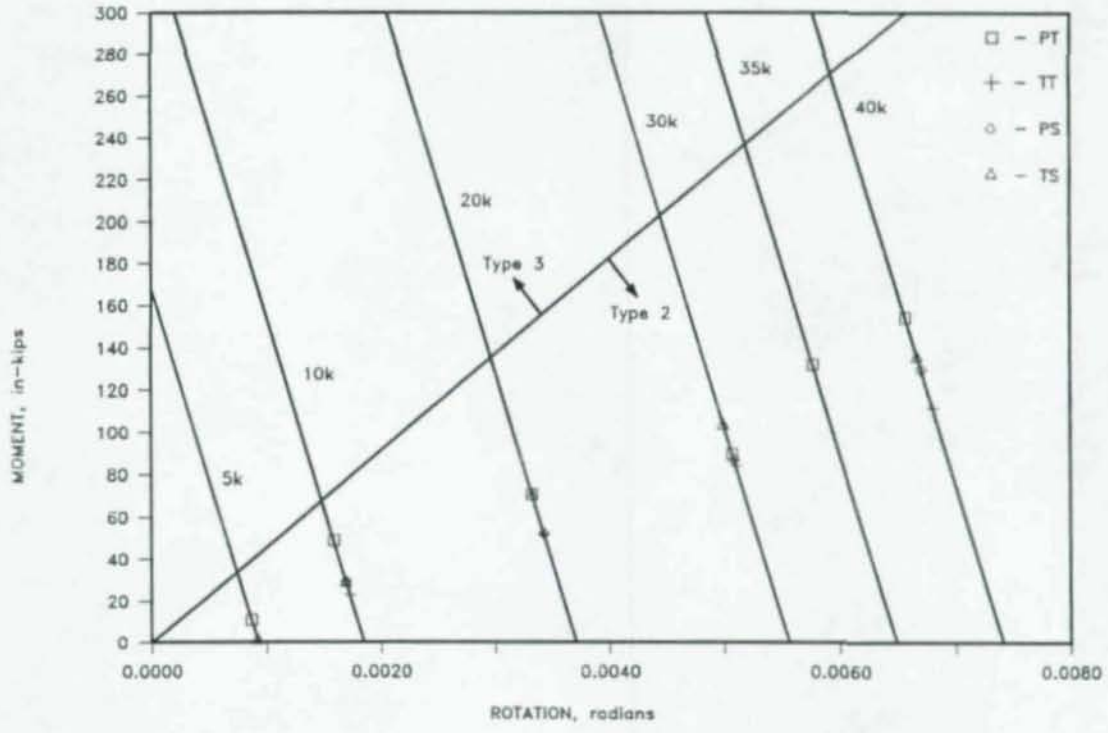

Figure 6.4: Beam-Line Plot Enlarged

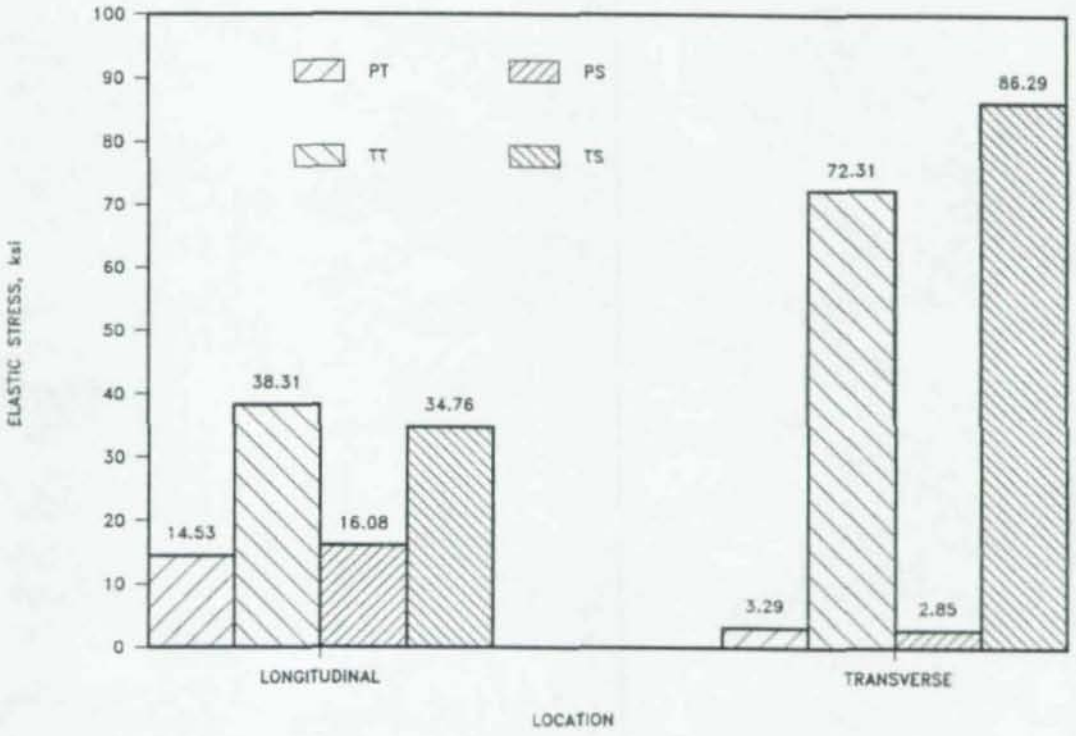

Figure 6.5: Tube Wall Stresses @ 30k Reaction

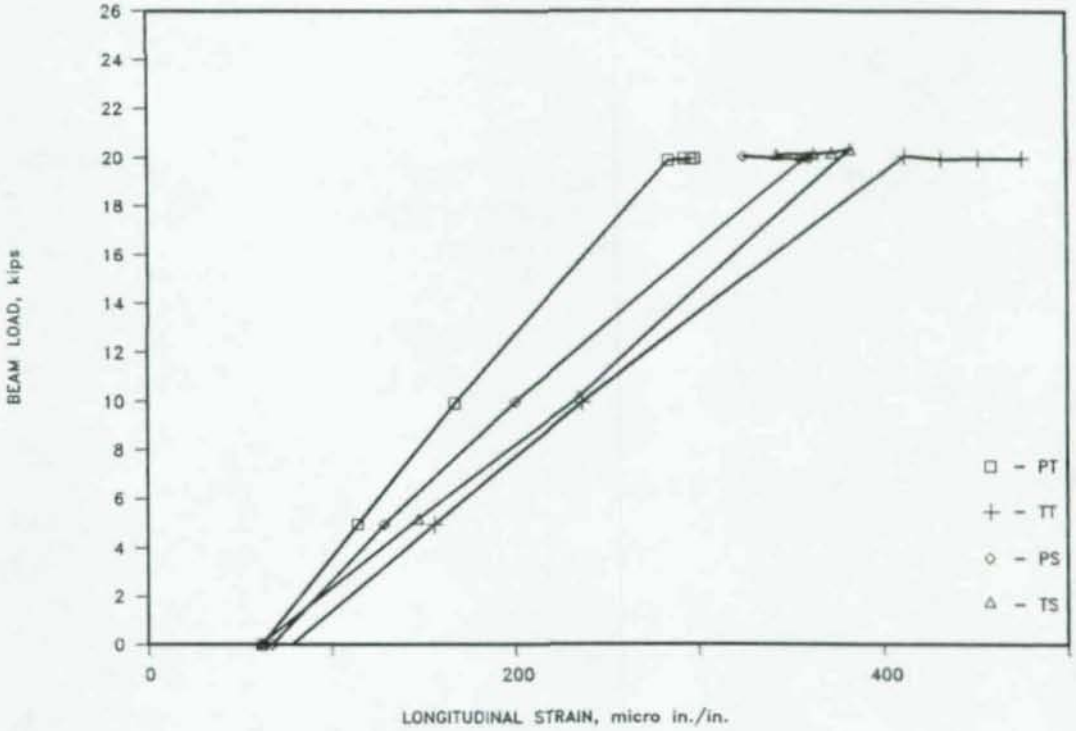

Figure 6.6: P_{beam} vs. $\in_{long}$ – Unbalanced Load Condition

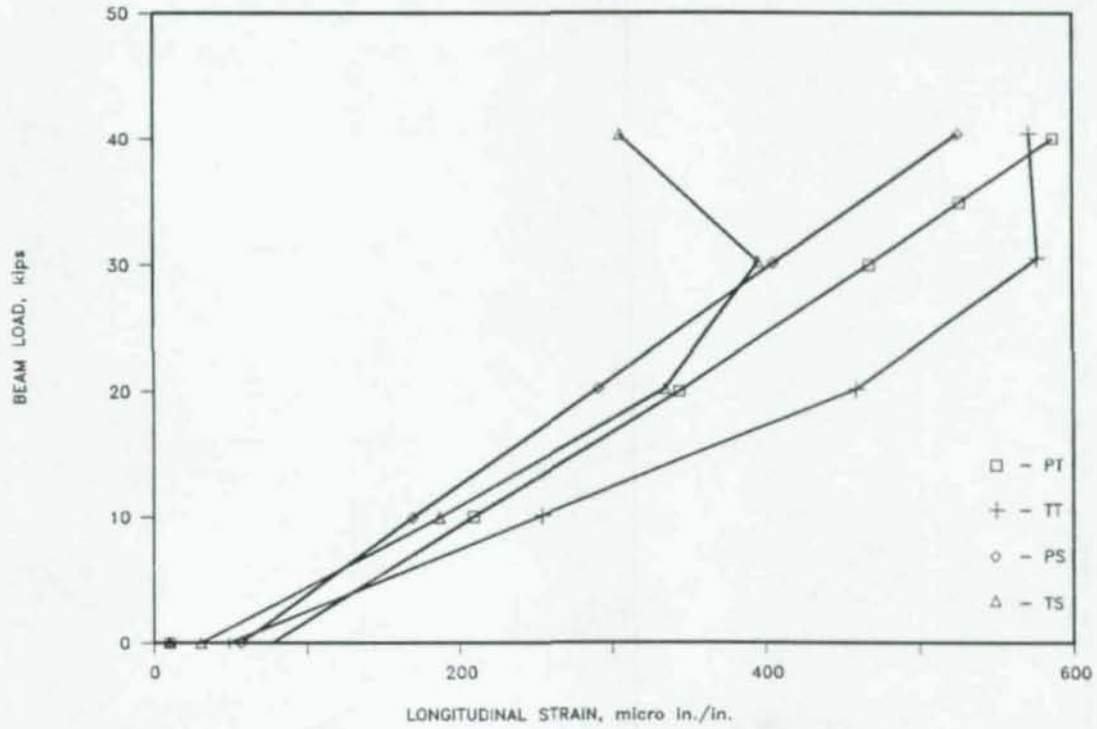

Figure 6.7: P_{beam} vs. $\in_{long}$ – Balanced Load Condition

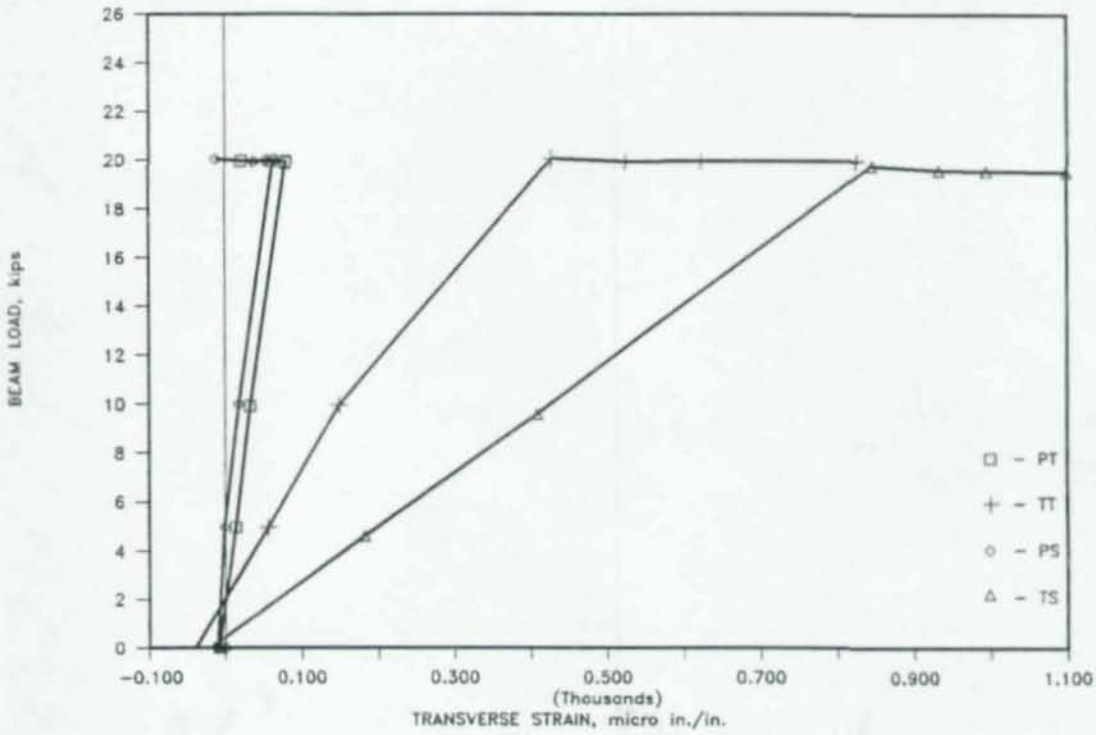

Figure 6.8: P_{beam} vs. ϵ_{tran} – Unbalanced Load Condition

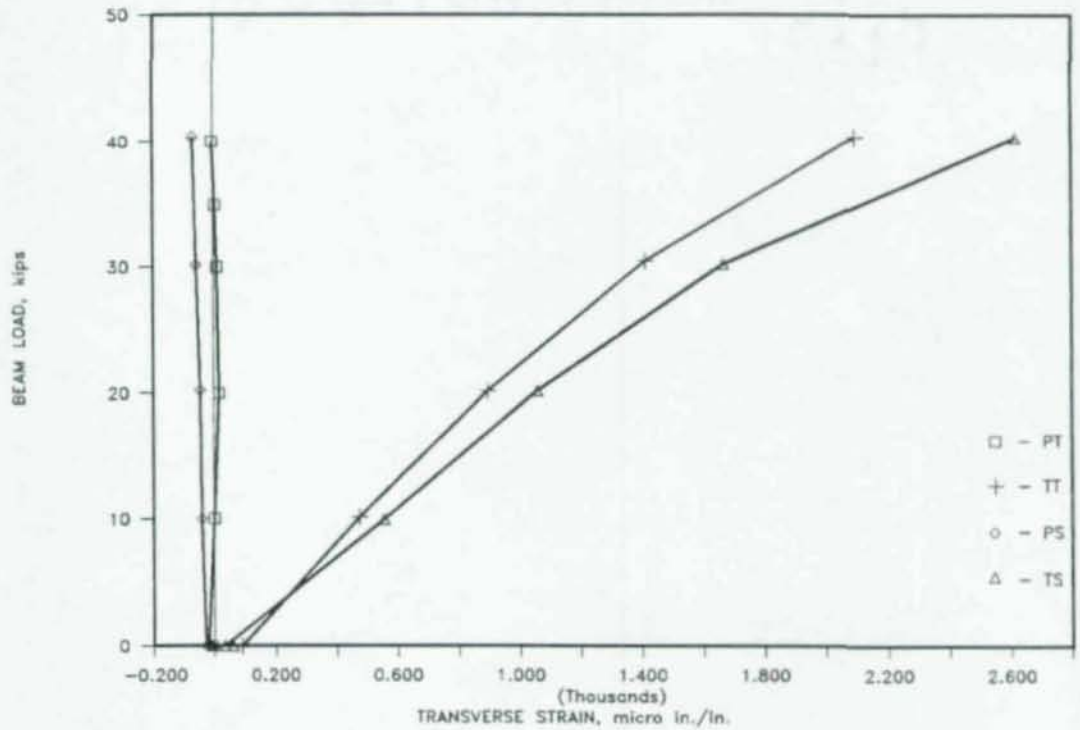

Figure 6.9: P_{beam} vs. ϵ_{tran} – Balanced Load Condition

7. COLUMN BEHAVIOR

7.1 Experimental Results

The load versus displacement plots of the four tests are shown in Figures 7.1, 7.2, and 7.3. These figures are column load versus lateral displacement plots at the middle of each segment and at the connection. Also listed in Figure 7.1 are the ultimate loads for each of the four tests.

Table 7.1 is a list of the theoretical and the experimental effective length factors for the four tests. The experimental effective length factors were determined from Southwell Plots for each of the four tests. The slope of the Southwell plot is defined as 1/Q, where Q is the Euler buckling load. From Eqn. 2.1 and the Euler buckling loads obtained from the Southwell Plots the experimental effective length factors were determined. The theoretical effective length factors were determined by performing a column stability analysis as presented in Section 2.1.3 of this paper. Here the effective length factors were determined for the ratio of connection load to the load applied at the top of the column(the term α in Table 7.1). Refer to Appendices B and C for the procedures used in the determination of the theoretical and experimental effective length factors used in this investigation.

In addition to the information listed above, Figures 7.4 to 7.7 are column load versus strain plots for each of

the four tests. Figures 7.4 and 7.5 are plots of column load in the lower segment versus longitudinal strain that occurred in the tube wall one-inch below the connection plates for the North and South sides, respectively. Figures 7.6 and 7.7 are plots of column load in the lower segment versus transverse strain in the tube wall one-inch below the connection plates for the North and South sides, respectively.

7.2 Discussion of Results

The experimental column capacities of the four tests range from 160 to 170 kips as presented in Figure 7.1. However, the capacity based on design Eqn. 2.10 for the test specimens is 152 kips using an average yield strength of 65 ksi and an average effective length factor of .896. The experimental capacities are well above the theoretical capacity which indicates that there is some conservatism in the design equation. However, normal scatter in data can be expected since the design equation is a selected average of the several column curves.

The experimental capacities for the PT and TT specimens in comparison with the PS and TS specimens indicate that the use of the shear tab connection does not significantly affect the capacity of tubular columns in comparison with the through plate connection. The capacities for the PT and TT specimens are 170 and 166 kips, respectively and the capacities for the PS and TS specimens are 161 and 160 kips,

respectively. More important, the specimens with tight bolts, PT and TT, achieved somewhat higher capacities than the specimens with snug-tight bolts, PS and TS. Therefore, the method of bolt tightening has more of an impact on the column capacity of tubular columns than the use of the shear tab connection.

For the test specimens in this investigation, the use of the shear tab connection did not significantly affect the capacity of rectangular-tubular columns in comparison with the through plate connection. However, the capacity of tubular columns with different slenderness ratios and w/t ratios than the specimens of this investigation may be affected by rotational distortion caused by the shear tab connection. The distortion in the tube wall that results from the shear tab connection may not significantly affect the capacity of long columns since they tend to fail elastically. On the other hand, the shear tab connection may reduce the capacity of short columns. Since the capacity of short columns is affected by geometric imperfections and residual stress, it is reasonable to assume that the local distortion caused by the shear tab may reduce their capacity. However, the effect of shear tab connections on tubular column strengths requires further study to determine if the capacities of other tubular sections are reduced. Therefore, the results obtained are limited to the specimens tested in this investigation.

Specimen	K_{exp}	$\alpha=P_c/P_{ax}$	K_{theor}
PT	.890	.542	.924
TT	.898	.564	.922
PS	.893	.611	.918
TS	.903	.603	.919
Ave	.896		.921

Table 7.1: Effective Length Factors

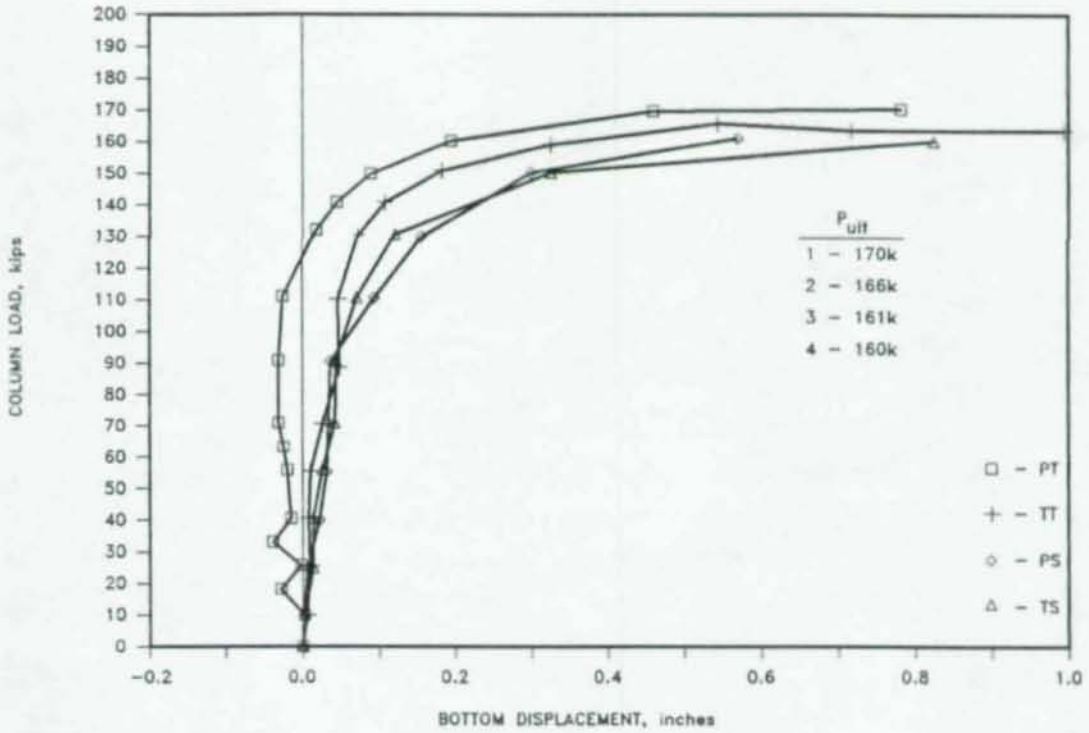

Figure 7.1: P_{col} vs. δ_{bottom}

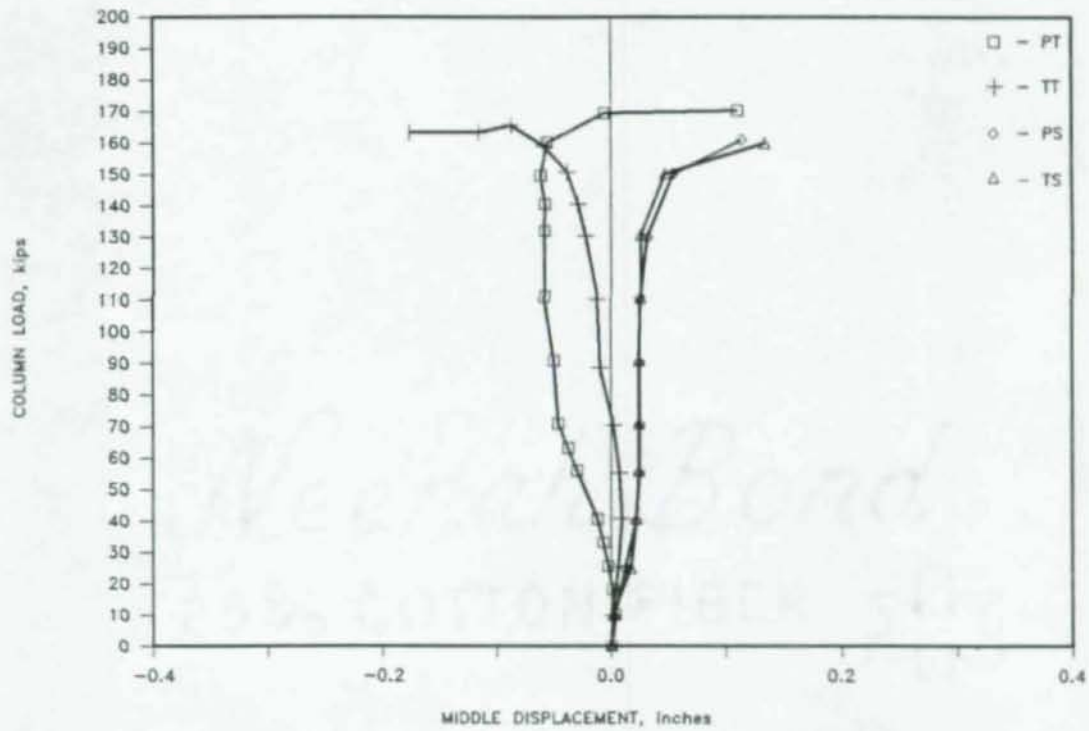

Figure 7.2: P_{col} vs. δ_{middle}

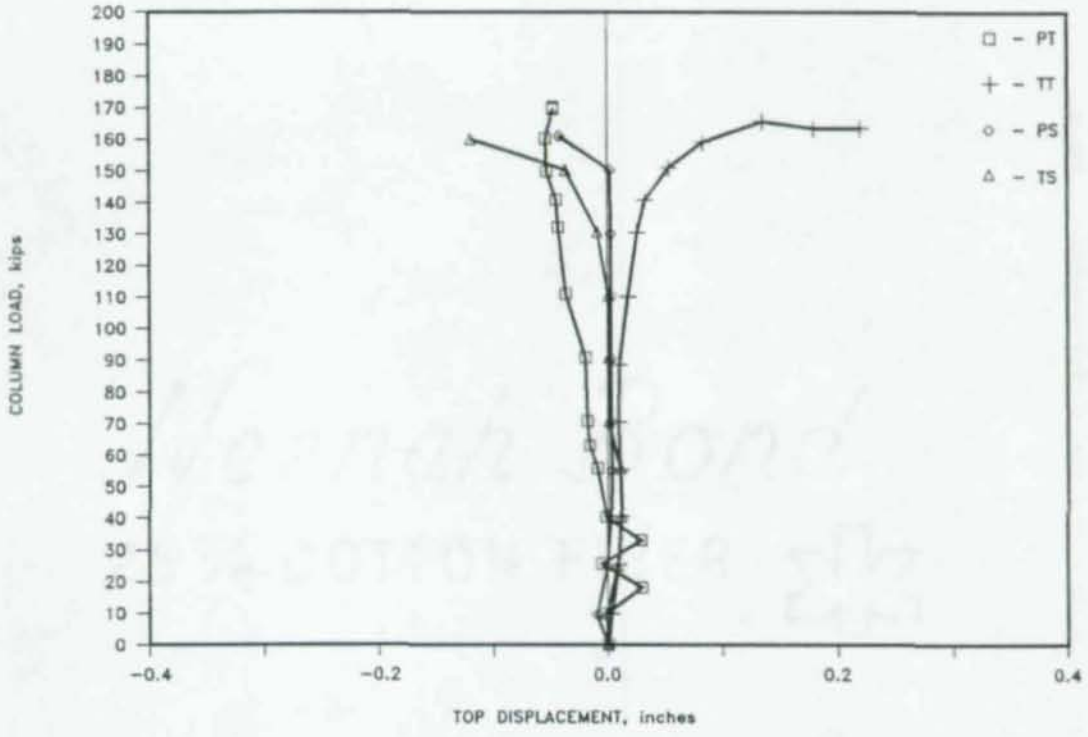

Figure 7.3: P_{col} vs. δ_{top}

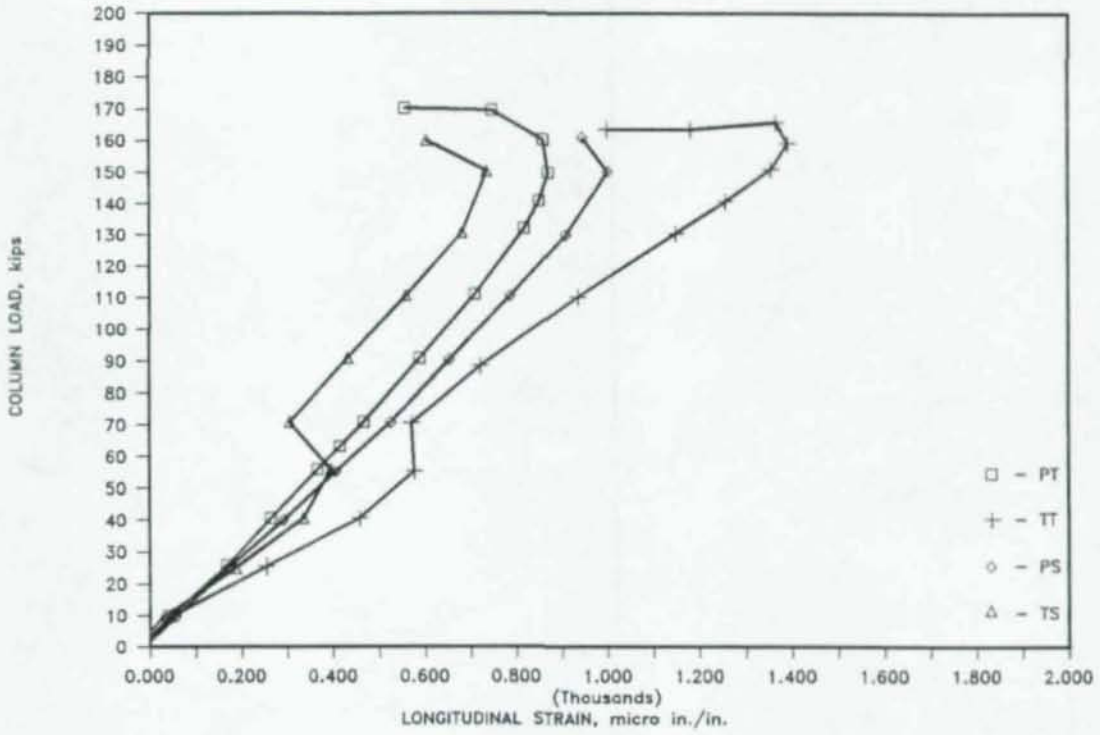

Figure 7.4: P_{col} vs. ϵ_{long} – North Side

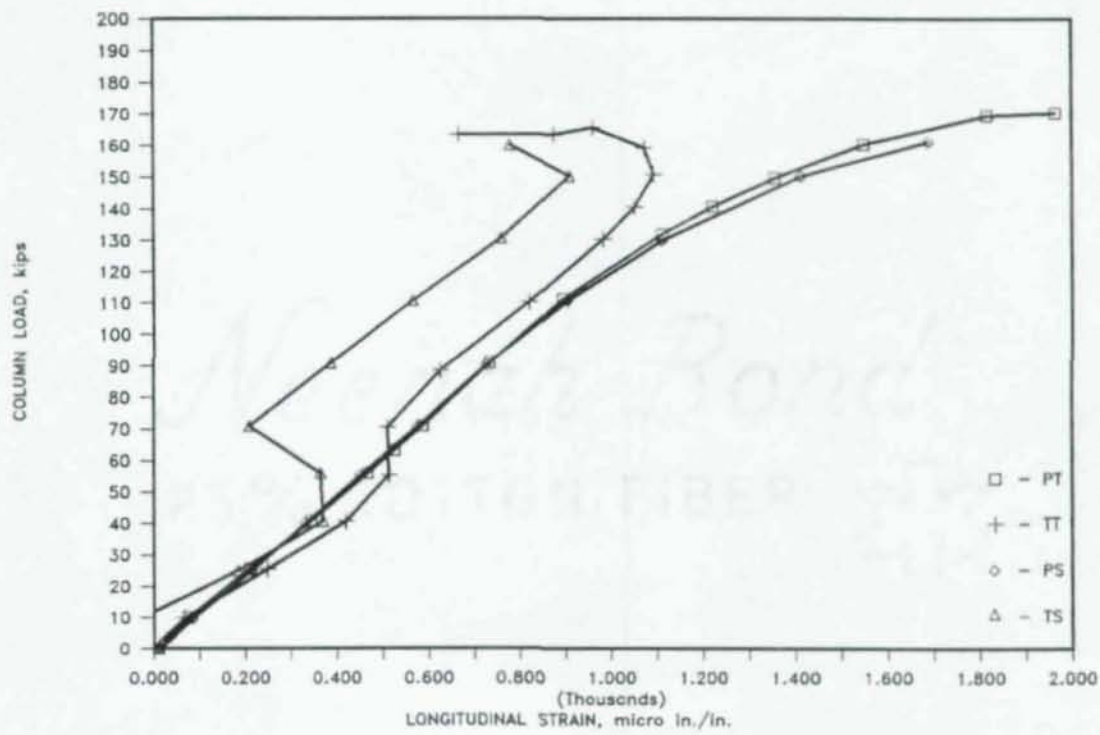

Figure 7.5: P_{col} vs. ϵ_{long} – South Side

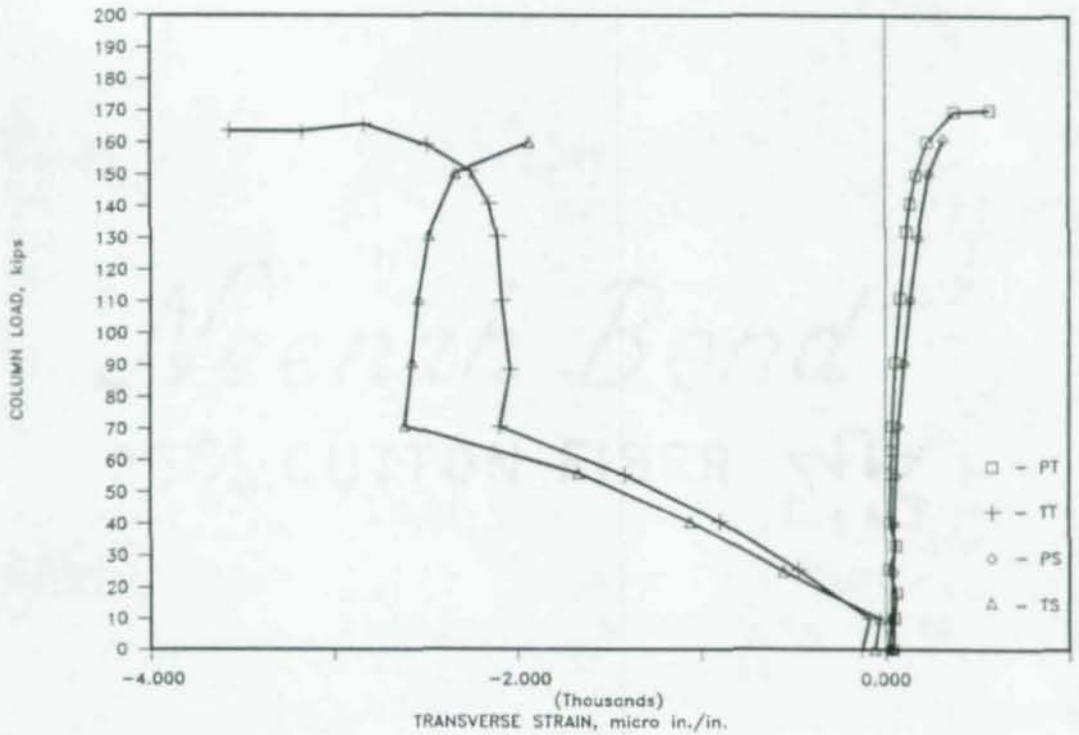

Figure 7.6: P_{col} vs. ϵ_{trans} – North Side

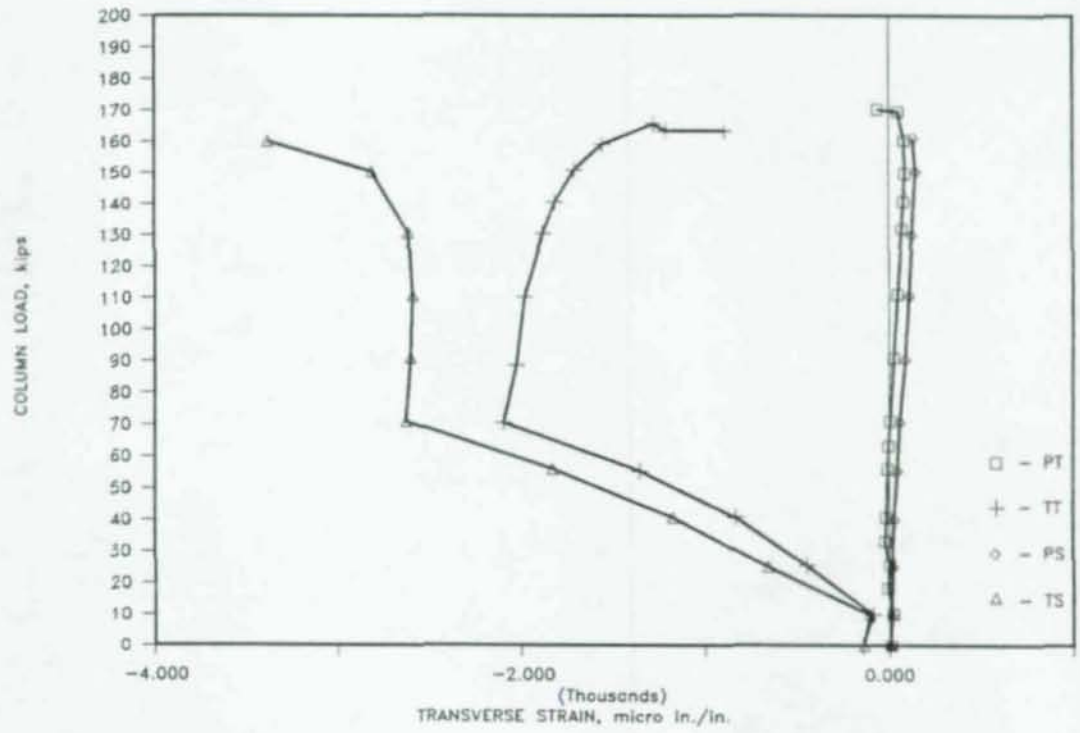

Figure 7.7: P_{col} vs. ϵ_{trans} – South Side

8. CONCLUSIONS AND RECOMMENDATIONS

8.1 Conclusions

Based on the results and test information contained in this paper the following conclusions are made:

1. The shear tab connection does not significantly reduce the capacity of rectangular-tubular columns in comparison with that of the through plate connection.
2. The method of bolt tightening had a greater affect on the column capacity than the use of the shear tab connection.
3. The moment-rotation characteristics of the shear tab connection and the through plate connection indicate that they perform in the range considered as simple "Type 2" connections.
4. There was a significant increase in transverse strain in the tube wall of the columns with shear tab connections in comparison with the columns that have through plate connections.

8.2 Recommendations

Although the shear tab connection did not significantly reduce the capacities of the rectangular-tubular columns in this investigation, additional research is necessary to determine if the capacities of other tubular columns of

various slenderness ratios and w/t ratios are affected by this connection.

Additional research is needed in order to obtain a design procedure for shear tabs welded to tubular columns. This procedure should take into consideration the affect of various w/t ratios; various beam sizes and spans; and the local bending of the tube wall. However, the design procedure for shear tabs welded to stiff supporting elements may be used in the design of shear tabs that are welded to tubular columns if the local bending of the tube wall is considered. This procedure will be conservative since the design moment in the shear tab will be greater than the actual moment in the connection due to the relative stiffness of the tube wall. Shear tabs should only be used in framing systems where the rotation in the connection is self-limiting.

REFERENCES

1. Richard, Ralph M., et al. "The Analysis and Design of Single Plate Framing Connections," AISC Engineering Journal, American Institute of Steel Construction, Chicago, 2nd Quarter, Vol. 17, No. 2, 1980.

2. Johnston, Bruce G., ed. Guide to Stability Design Criteria for Metal Structures, John Wiley & Sons, New York, 1976, pp. 26-68.

3. AISC Manual Committee. Manual of Steel Construction, Eighth Edition. Chicago: American Institute of Steel Construction, 1980.

4. Salmon, Charles G., and John E. Johnson. Steel Structures: Design and Behavior, Second Ed., Harper & Row, New York, 1980, pp. 251-279, 731, 732.

5. Chajes, Alexander, et al. Principles of Structural Stability Theory, Prentice-Hall, New Jersey, 1974, pp. 61-69.

6. Yu, Wei-Wen. Cold-Formed Steel Design, John Wiley & Sons, New York, 1985, pp. 226-246.

7. Weaver, William Jr. and James M. Gere. Matrix Analysis of Framed Structures, Second Edition, Van Nostrand Reinhold, 1980, pp. 417-420.

8. Gregory, Malcolm. Elastic Instability: Analysis of Buckling Modes and Loads of Framed Structures, E. & F.N. Spon Limited, 1967, pp. 138-154.

9. Bleich, Friedrich and Han H. Bleich, ed. Buckling Strength of Metal Structures, McGraw-Hill, 1952, pp. 1 -56.

10. Sherman, Donald R. Tentative Criteria for Structural Applications of Steel Tubing and Pipe, Washington, D.C.: Committee of Steel Pipe Producers, American Iron and Steel Institute, 1976, pp. 6-9, 30-35.

11. Engineering For Steel Construction, Chicago: American Institute of Steel Construction, 1984, pp. 3-51 to 3-54 and Appendix C.

12. Sherman, Donald R. "Bending Capacity of Fabricated Pipe at End Conditions," API Project Report 54258.09, April 1987.

APPENDIX A: CONNECTION DESIGN AND SELECTION

In this appendix the design of the shear tab connection is presented. With the assumption shown below and design aids from the publication "Engineering for Steel Construction[11]" a connection was selected. Any tables and/or figures used from this publication are reprinted at the end of this appendix.

Major assumption: Due to the flexibility of the column wall the eccentricity will be assumed to occur at the bolt line, three inches from the face of the wall of the column.

Given: R = 40 kips

e = 3 inches

bolts = 3/4 in. diam. A325-X

F_y = 36 ksi

F_u = 58 ksi

beam: W12 X 53

Find: The size of plate and the weld thickness needed.

Solution:

1. No. of bolts:

   n = 40/13.3

   = 3. USE 3 bolts

2. Beam requirements:

   a. minimum edge distance:

$$l_e = 2P/F_u t_w$$

$$= [2(40)]/[(3)(58)(.345)]$$

$$= 1.33 \text{ in.} \qquad \underline{\text{USE } l = 1.5 \text{ in.}}$$

   b. minimum bolt spacing:

$$s = 2P_r/F_u t_w + d/2$$

$$= 1.33 + .375$$

$$= 1.71 \text{ in.} \qquad \underline{\text{USE } s = 3 \text{ in.}}$$

3. Moment in shear tab at the face of the column:

$$M = 40(3.0)$$

$$= 120 \text{ in. kips}$$

4. Entering Table 3B of the AISC construction manual: For a moment of 120 inch-kips and a shear force of 40 kips, select a plate thickness of 5/16 inch and the fillet weld of 5/16 inch which has a shear capacity of 40 kips and a moment capacity of 152 inch-kips.

Table 3B. Maximum Permissible Beam End Reaction (kips)

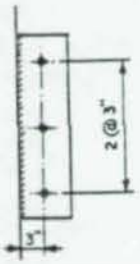

No. of Bolts: 3
Plate Depth: 9 in.

Min. Plate t, in.	Max Moment M, kip-in.	Fillet Weld Size (E70XX), in.									
		1/8	5/16	3/16	7/16	1/2	9/16	5/8	11/16
5/16	68	14	24						
	75	2	24						
	82		24						
	91		24						
1/4	100		23	32					
	107		15	32					
	114			32					
	122			32					
5/16	130			33	40				
	137			27	40				
	144			19	40				
	152				40				
3/8	160				43	48			
	167				38	48			
	174				31	48			
	182				20	48			
7/16	190					53	56		
	197					48	56		
	204					42	56		
	213					33	56		
1/2	220					22	64	64	
	227						59	64	
	234						53	64	
	243						44	64	
9/16	250						36	72	
	257						25	69	72
	264							63	72
	273							55	72
5/8	280							48	81
	288							38	78	81
	296							23	72	81
	304								66	81
11/16	310								60	89
	318								51	89	89
	326								40	83	89
	334								23	76	89

Max. Permissible Plate Thickness, in.		
Bolt		Plate
Type	Diam.	Max. t
A325	3/4	3/8
	7/8	7/16
	1	9/16
A490	3/4	1/2
	7/8	5/8
	1	11/16

Note: For standard holes only; restriction does not apply for bolts in slotted holes.

Note: 1. Where no maximum permissible beam end reaction is tabulated, the connection is invalid.
2. Plate material: A36 steel.

APPENDIX B: THEORETICAL COLUMN CAPACITY

B.1 Effective Length Determination

The effective length factor for a two-story continuous column can be determined by performing a column stability analysis using flexural stiffness functions modified by an axial force. This section of Appendix B illustrates the procedures used to determine the theoretical effective length factor for the column used in this investigation.

Given: $L_1 = L_2 = L = 10' = 120"$

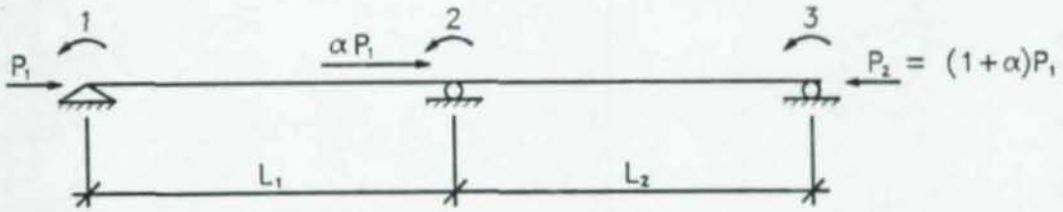

From Figure 2.2 the stiffness matrix for the free degrees of freedom, S_{FF}, is

$$S_{FF} = EI \begin{bmatrix} C_3 & C_4 & 0 \\ C_4 & C_3+C_7 & C_8 \\ 0 & C_8 & C_7 \end{bmatrix}$$

The column becomes unstable when the determinant of the stiffness matrix approaches zero. The critical loads of the column are determined by setting the determinant of the stiffness matrix equal to zero and solving for the unknowns. The determinant of the stiffness matrix is

$$\text{DET } S_{FF} = C_3(C_3+C_7)C_7 - C_8^2C_3 - C_4^2C_7 \qquad (B.1)$$

where: $C_3=4S_{31}/L_1$, $C_4=2S_{41}/L_1$, $C_7=4S_{32}/L_2$, $C_8=2S_{42}/L_2$,

$S_{31}=T_1[\sin(T_1)-T_1\cos(T_1)]/4\phi_1$,

$S_{41}=T_1[T_1-\sin(T_1)]/2\phi_1$, $S_{42}=T_2[T_2-\sin(T_2)]/2\phi_2$,

$S_{32}=T_2[\sin(T_2)-T_2\cos(T_2)]/4\phi_2$, $T_1=(L_1)(P_1/EI)^{0.5}$,

$T_2=(L_2)(P_2/EI)^{0.5}$, $\phi_1=2-2\cos(T_1)-T_1\sin(T_1)$, and

$\phi_2=2-2\cos(T_2)-T_2\sin(T_2)$.

With the substitution of the terms listed above into Eqn. B.1, there are two unknowns T_1 and T_2. Solving for T_1 and T_2, axial loads P_1 and P_2 can be determined at which the system becomes unstable. From these axial loads the effective length factors can be determined from Euler buckling theory using Eqn. 2.1 if the length, L, is replaced by the effective length, KL. However, there are two unknowns and one equation. Another equation must be obtained to solve for T_1 and T_2. From compatibility,

$$T_1=(L_1)\ [P_1/EI]^{0.5} \qquad (B.2)$$

and

$$T_2=(L_2)\ [(1+\alpha)P_1/EI]^{0.5} \qquad (B.3)$$

By rearranging terms,

$$T_2=T_1\ [1+\alpha]^{0.5} \qquad (B.4)$$

Now Eqn. B.1 can be solved by a trial and error procedure for values of T_1 and T_2 for which the column becomes

unstable. From Euler theory, Eqn. 2.1 using an effective length,

$$K_i=(1/L_i)\ [\pi^2 EI_i/P_i]^{0.5} \qquad (B.5)$$

and from Eqn. B.1

$$T_i=(L_i)\ [P_i/EI_i]^{0.5}$$

Therefore,

$$K_i= \pi/T_i \qquad (B.6)$$

Elastic effective length factors were determined for alpha values ranging from 0 to 1.0 as shown below.

α	K_1	K_2
.0	1.000	1.000
.1	1.027	.979
.2	1.052	.961
.3	1.080	.947
.4	1.106	.935
.5	1.134	.926
.6	1.161	.918
.7	1.190	.913
.8	1.215	.906
.9	1.242	.901
1.0	1.269	.898
Ave.	1.134	.935

B.2 Theoretical Column Capacity

The calculation of the expected column capacity of the test specimens is based on the information presented above and the equations presented in Section 2 of this paper.

Given: $K_{ave} = 0.935$

$L = 10$ ft.

$F_y = 57.3$ ksi (Based on the mill report)

$r_y = 1.18$ in.

$A_g = 4.98$ sq. in.

Solution:

1. Flat width to thickness ratio:

   $w/t = 6/.3125 = 19.2$

   $238/\sqrt{F_y} = 238/\sqrt{57.3} = 31.4$ o.k.

2. Slenderness ratio:

   $KL/r = [(0.935)(10)(12)]/(1.18) = 94.6$

   $C_c = 925/\sqrt{F_y} = 925/\sqrt{57.3} = 122.2$

   Use Eqn. 2.3 from Section 2.1.5 for Class B tubes.

3. Stress equation:

   $Fa = \{1-(KL/r)/(1.5C_c)\}F_y$

   $= \{1-(94.6)/[1.5(122.2)]\}57.3$

   $= 27.73$ ksi

4. Ultimate load:

$$P = A_g F_a$$

$$= 4.98(27.73)$$

$$= 138 \text{ kips}$$

The ultimate load of the test specimens is 138 kips for a yield strength of 57.3 ksi and an average effective length factor of .935.

APPENDIX C: COLUMN CAPACITY ANALYSIS

C.1 Effective Length Determination

The actual effective length factor must be determined in order to evaluate the buckling behavior of the test specimens. A method of determining the effective length factor, K, is to graph Southwell plots for each of the four tests as explained in Section 2.2 of this paper. The Southwell Plots for the four tests are shown in Figures C.1 to C.4 at the end of this appendix. The slope of the best fit line through the data points is 1/Q, where Q is the Euler buckling load of the column. From this buckling load an elastic effective length factor was determined using Euler's elastic buckling equation using KL in place of L. The following table shows the effective length factors and the buckling loads for each of the four tests.

specimen	slope	intercept	Q	K
PT	.005720	.000103	175	.890
TT	.005809	.000215	172	.898
PS	.005734	.000283	174	.893
TS	.005876	.000281	170	.903
Ave	.005785	.000220	173	.896

C.2 Column Capacity

This section of Appendix C presents the calculation of the experimental column capacity using the information listed above and the equations from Section 2 of this paper.

Given: $K_{ave} = 0.896$

$L = 10$ feet

$F_y = 65$ ksi

$r_y = 1.18$ in.

$A_g = 4.98$ sq. in.

Solution:

1. Flat width to thickness ratio:

$w/t = 6/.3125$

$= 19.2$

$238/\sqrt{F_y} = 238/\sqrt{65}$

$= 29.5$ o.k.

2. Slenderness ratio:

$KL/r = (.896)(10)(12)/1.18$

$= 91$

$C_c = 925/\sqrt{65}$

$= 114.7$ o.k.

3. Axial stress:

$$F_a = [1 - (KL/r)/1.5C_c]F_y \qquad (2.13)$$

$$= \{1 - 91/[(1.5)(114.7)]\}(65)$$

$$= 30.57 \text{ ksi}$$

4. Axial load:

$$P = A_g F_a$$

$$= (4.98)(30.57)$$

$$= 152 \text{ kips}$$

The axial load as determined by Eqn. 2.13 is 152 kips for a yield strength of 65 ksi and an average effective length of .896.

C.3 Initially Curved Column Behavior

If the center line of a pinned column under an axial load P is defined by y(x) and having an initial out-of-straightness given by $y_o(x)$,

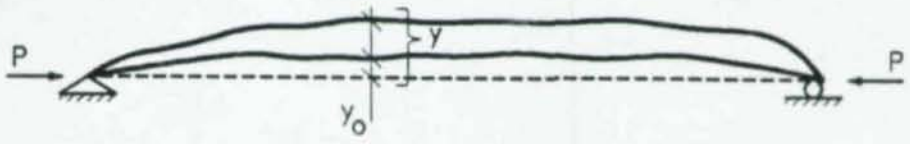

the bending moment at x is

$$M = Py$$

where

$$Py = -EId^2(y-y_o)/dx^2$$

$$= -EI(d^2y/dx^2) + EI(d^2y_o/dx^2)$$

therefore the differential equation is

$$(d^2y/dx^2) + (P/EI)y = (d^2y_o/dx^2) \qquad (C.1)$$

The form of $y(x)$ is dependent on the form of $y_o(x)$. Assume $y_o(x)$ to have the form of

$$y_o = \sum a_n \sin(n\pi x/l)$$

and

$$y = \sum b_n \sin(n\pi x/l)$$

Substituting $y(x)$ and $y_o(x)$ in the Eqn. C.1 the differential equation becomes

$$\sum[(-n^2\pi^2 b_n/l^2) + k^2 b_n]\sin(n\pi x/l) = \sum(-n^2\pi^2 a_n/l^2)\sin(n\pi x/l) \qquad (C.2)$$

where $k = (P/EI)^{0.5}$. Eqn. C.2 applies for all x, therefore

$$(b_n - a_n)n^2\pi^2/l^2 = k^2 b_n$$

and

$$b_n = a_n/(1-k^2l^2/n^2\pi^2) \qquad (C.3)$$

The first Euler load of the column is defined as

$$Q = \pi^2 EI/l^2.$$

Therefore

$$b_n/a_n = (1-P/n^2Q)^{-1}$$

giving the ratio in which the initial shape $a_n \sin(n\pi x/l)$ is magnified by the axial force, P. As P approaches Q

$$b_1/a_1 = \infty,$$

$$b_2/a_2 = 4/3,$$

$$b_3/a_3 = 9/8, \text{ etc.}$$

The central deflection of the column, x = 1/2, is

$$b = b_1 - b_3 + b_5 - b_7 + \ldots$$

As P approaches Q, the terms after b_1 can be neglected, therefore

$$b = b_1 = a_1/(1-P/Q)$$

provided that the curvature is small and yielding does not occur. The measured central deflection of test columns is

$$\begin{aligned} \delta &= b - y_o \\ &= b - a_1 \\ &= [a_1/(1-P/Q)] - a_1. \end{aligned}$$

This equation reduces to

$$\delta/P = \delta/Q + a_1/Q \qquad (C.4)$$

The term a_1/Q is constant for the column knowing the initial deflection of the column at its midheight[8]. A generalized plot of Eqn. C.4 is shown in Figure 2.3.

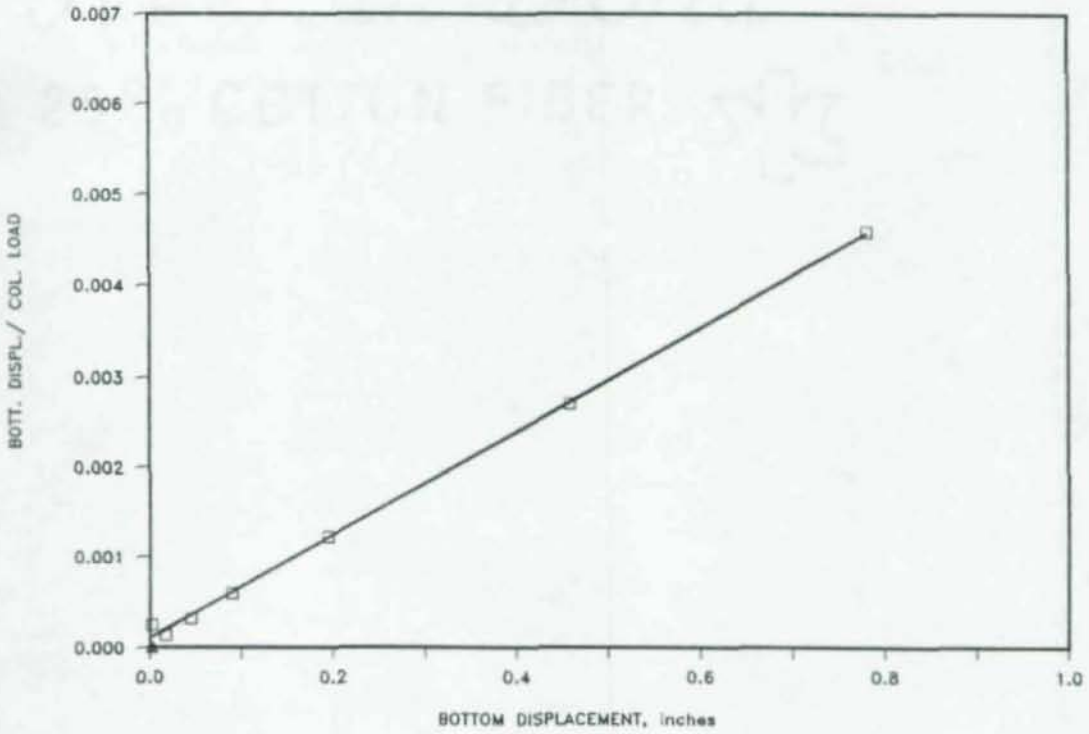

Figure C.1: Southwell Plot – Test 1 – PT

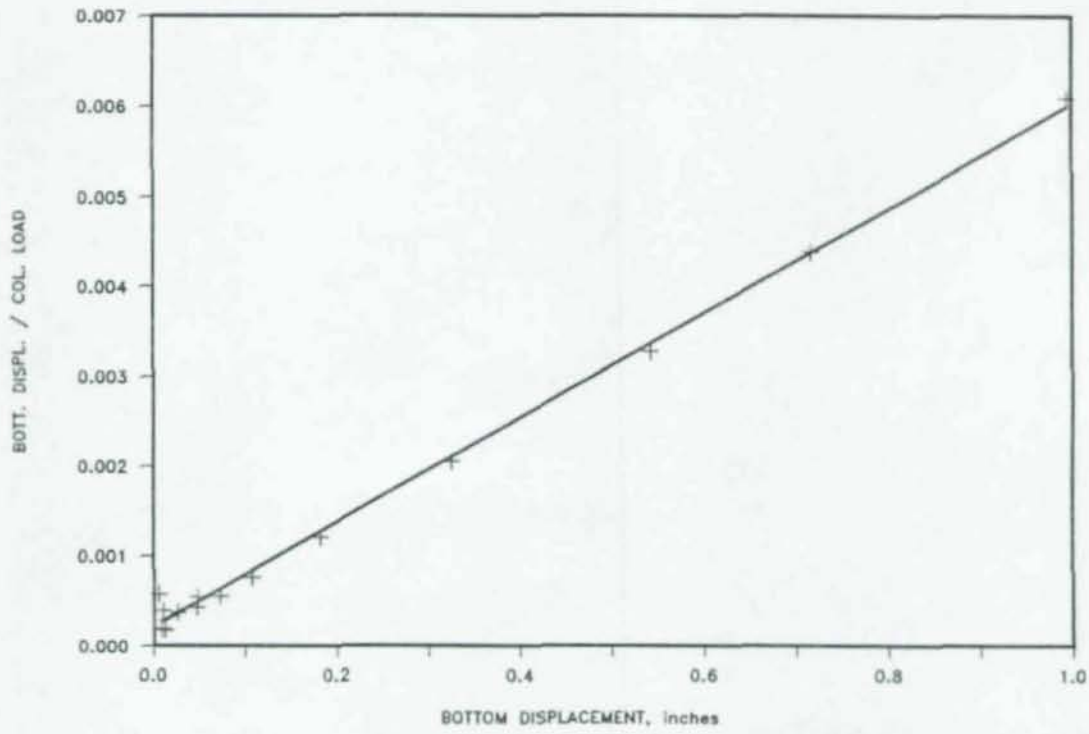

Figure C.2: Southwell Plot – Test 2 – TT

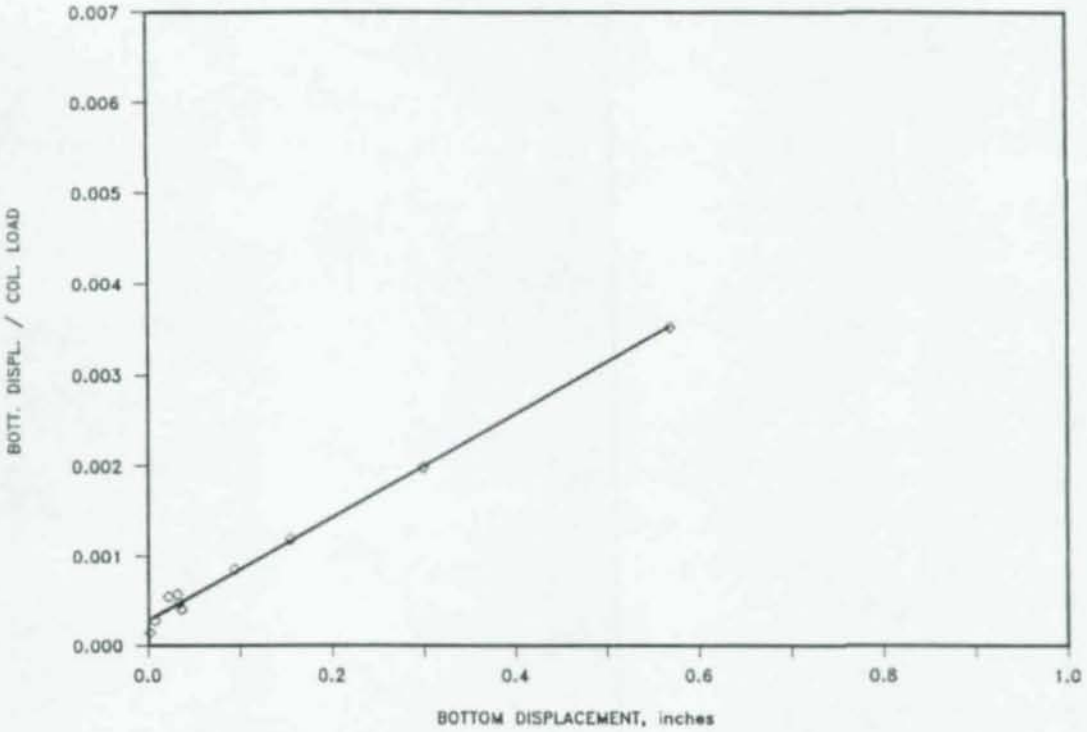

Figure C.3: Southwell Plot – Test 3 – PS

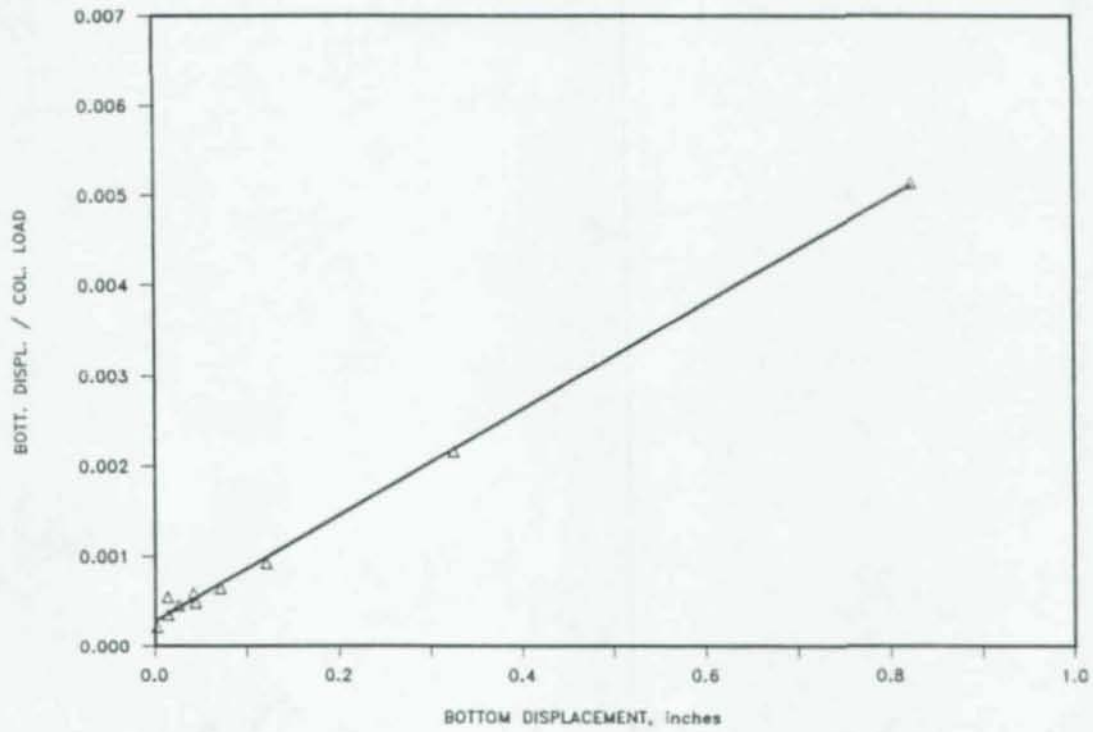

Figure C.4: Southwell Plot – Test 4 – TS

APPENDIX D: ECCENTRICITY ANALYSIS

In this appendix a sample calculation for the load eccentricity is presented for a beam reaction of 30 kips. Also the theoretical eccentricity as determined by Reference 1 is presented. The eccentricities determined in this appendix are measured with respect to the bolt line.

D.1 Experimental Eccentricity

The moment in the connection is determined by using the linear strain gages that were mounted to the connection plates as shown in Figure 4.5.

$$M_{conn} = .0612(\epsilon_T + \epsilon_B) \qquad (4.1)$$

and

$$e_{conn} = M_{conn}/V_{beam} - 2.375 \qquad (4.2)$$

where: ϵ_T = strain in the top of plate, μin./in.

ϵ_B = strain in bottom of plate, μin./in.

$V_{beam} = P_{beam} - R_{beam}$, kips

P_{beam} = beam load, kips

R_{beam} = beam reaction, kips

Example: Test 1 North Side

Given: ϵ_T = 1176 μin./in.

ϵ_B = -957 μin./in.

P_{beam} = 40.01 kips

R_{beam} = 9.87 kips

a = 4.5 feet

L = 17 feet

Solution:

1. The moment in the connection is

M_{conn} = .0612 [1176 - (-957)]

= 130.5 in. kips

2. The shear in the connection is

V_{beam} = 40.01-9.87

= 30.14 kips

3. The eccentricity in the connection is

e_{conn} = 130.5/30.14 - 2.375

= 1.95 in.

D.2 Theoretical Eccentricity

This part of Appendix D is devoted to the calculation of the theoretical eccentricity as presented in Reference 1. Any figures used from this reference are reprinted for convenience.

Given: W12X53 beam

3-3/4 in. diam. A325-X bolts

L = 17 feet

1. $L/d = [(17)(12)]/[(12.06)] = 17$

2. The number of bolts = 3

3. $(e/h)_{ref} = 0.06(1/d) - 0.15$

$= 0.06(17) - 0.15$

$= 0.87$

$e(S)^{0.4} = h(e/h)_{ref} * n/N * (S_{ref})^{0.4}$

$= 6(0.87) * 3/5 * 100^{0.4}$

$= 19.76$

4. $e = [e(S)^{0.4}]/(S)^{0.4}$

$= 19.76/(70.6)^{0.4}$

$= 3.60$ in.

This is the eccentricity for a uniformly loaded beam.

5a. Here the eccentricity for a uniformly loaded beam is modified to the eccentricity of the concentratedly loaded beam. The moment rotation curve of a beam is essentially flat when it is loaded to its first yield load. Therefore, the moment in the connection can be considered independent of rotation[1].

5b. Eccentricity for a uniformly loaded beam:

Assuming W_y is the first yield uniform load

$$M_{beam} = (1/8)(W_y)(L^2) = (F_y)(S)$$

and

$$V_{beam} = (W_y)(L)/2 = 4(F_y)(S)/L$$

Therefore,

$$e_{uniform} = (M_{conn})(L)/4(F_y)(S)$$

5c. Eccentricity for a concentratedly loaded beam:

Assuming P_y is the first yield concentrated load

$$M_{beam} = (P_y)(a)(b)/L = (F_y)(S)$$

and

$$V_{beam} = (P_y)(b)/L = (F_y)(S)/a$$

Therefore,

$$e_{conc} = (M_{conn})(a)/(F_y)(S)$$

5d. The eccentricity for the concentratedly loaded beam in terms of the eccentricity for a uniformly loaded beam is

$$\frac{e_{conc}}{e_{unif}} = \frac{a/L}{1/4} = \frac{4.5/17}{1/4}$$

Now,

$$e_{conc} = 1.06 * e_{unif}$$
$$= (1.06)(3.61)$$
$$= 3.83 \text{ in.}$$

Therefore, the theoretical eccentricity is 3.83 inches from the bolt line[1].

APPENDIX E: INDIVIDUAL TEST RESULTS

In this appendix the individual test results is provided for each of the four tests. The following information is provided for each test:

1. Data table consisting loads, displacements, and strains for the connection test and the column test.
2. A plot of the column load versus lateral displacement of the lower segment of the column.
3. A plot and photo of the buckled shape.

EAST LOAD (kips)	WEST LOAD (kips)	SOUTH LOAD (kips)	NORTH LOAD (kips)	SOUTH REACT. (kips)	NORTH REACT. (kips)	SOUTH SLOPE (milli-radians)	NORTH SLOPE	BOTT. DISP. (inches)	MIDL. DISP. (inches)	TOP DISP. (inches)	NORTH AXIAL	NORTH TRANS	NORTH TOP	NORTH BOTT.	SOUTH AXIAL	SOUTH TRANS	SOUTH TOP	SOUTH BOTT.
											(micro inch/inch)							
0.00	0.00	0.00	0.00	0.00	0.00	0.000	0.000	0.000	0.000	0.000	0	0	0	0	0	0	0	0
5.34	5.32	0.17	0.00	0.02	0.04	0.034	0.014	0.003	0.006	0.004	-61	8	61	129	-72	9	85	0
5.08	5.30	0.16	4.95	0.10	1.28	0.048	0.160	0.018	0.005	-0.008	-114	-14	163	-18	-83	7	177	0
5.10	5.06	0.17	9.92	0.15	2.52	0.072	0.956	0.036	0.004	-0.029	-167	-33	204	-105	-88	14	216	0
5.11	5.11	0.16	19.90	0.18	5.03	0.100	2.732	0.084	0.001	-0.081	-284	-79	360	-314	-89	48	206	0
5.01	5.08	5.03	19.94	1.16	4.97	-0.079	2.771	0.081	-0.002	-0.075	-297	-79	433	-390	-136	43	416	0
5.16	5.03	10.02	19.97	2.43	4.96	-0.826	2.817	0.066	-0.003	-0.058	-299	-62	483	-411	-191	33	620	0
5.03	5.05	19.97	19.98	4.89	4.92	-2.775	2.835	0.023	-0.006	-0.017	-293	-21	548	-408	-299	19	1017	0
4.86	4.84	20.03	10.90	5.02	2.71	-3.078	1.627	-0.018	-0.006	0.019	-190	18	381	-158	-280	13	940	0
4.98	4.92	20.05	0.01	5.08	0.11	-3.126	0.330	-0.074	-0.003	0.076	-60	73	232	20	-277	-14	922	0
5.11	5.31	10.18	0.01	2.69	0.02	-1.976	0.206	-0.046	0.001	0.054	-48	65	124	94	-179	4	524	0
4.98	5.02	0.10	0.01	0.13	0.08	-0.379	-0.043	-0.006	0.003	0.012	-50	26	29	123	-60	27	123	0
0.09	0.07	0.18	0.00	0.11	0.04	-0.327	0.000	-0.006	-0.002	0.010	8	20	-40	13	4	15	21	0

Table E.1: Connection Test Data - Test 1 - PT

EAST LOAD (kips)	WEST LOAD (kips)	SOUTH LOAD (kips)	NORTH LOAD (kips)	SOUTH REACT. (kips)	NORTH REACT. (kips)	SOUTH SLOPE (milli-radians)	NORTH SLOPE (milli-radians)	BOTT. DISP. (inches)	MIDL. DISP. (inches)	TOP DISP. (inches)	NORTH AXIAL (micro inch/inch)	NORTH TRANS (micro inch/inch)	NORTH TOP (micro inch/inch)	NORTH BOTT. (micro inch/inch)	SOUTH AXIAL (micro inch/inch)	SOUTH TRANS (micro inch/inch)	SOUTH TOP (micro inch/inch)	SOUTH BOTT. (micro inch/inch)
0.00	0.00	0.00	0.00	0.00	0.00	0.000	0.000	0.000	0.000	0.000	14	39	-68	37	-10	8	22	-36
5.13	5.13	-0.18	0.00	0.00	0.05	0.031	-0.021	0.002	0.004	-0.001	-44	46	-14	122	-75	19	116	73
5.32	5.26	9.96	-0.01	2.49	-0.14	-1.133	-0.256	-0.028	0.001	0.030	-59	55	131	-23	-189	-10	526	-287
5.41	5.22	9.99	9.96	2.40	2.46	-1.174	0.679	-0.002	-0.003	-0.005	-168	16	261	-260	-209	-0	662	-415
5.37	5.10	19.89	9.94	4.80	2.40	-2.754	0.892	-0.039	-0.007	0.029	-165	53	307	-295	-324	-23	1005	-706
5.21	5.02	19.98	20.15	4.78	4.97	-2.802	2.281	-0.015	-0.012	-0.001	-263	25	504	-524	-344	-16	1082	-822
5.26	5.26	30.01	30.08	7.21	7.43	-4.530	4.242	-0.020	-0.030	-0.009	-366	29	838	-730	-468	-10	1541	-1207
5.21	5.00	34.93	35.19	8.40	8.68	-5.201	5.261	-0.024	-0.038	-0.016	-416	32	1004	-843	-526	-4	1757	-1449
5.23	5.25	39.99	40.01	9.62	9.87	-6.441	5.993	-0.031	-0.046	-0.018	-467	37	1176	-957	-587	4	2018	-1700
15.21	14.95	39.98	40.27	9.61	9.95	-6.448	6.266	-0.031	-0.050	-0.020	-589	53	1258	-888	-733	26	2117	-1616
25.21	25.29	39.96	40.24	9.62	9.96	-6.465	6.341	-0.026	-0.058	-0.036	-711	81	1187	-864	-894	47	2044	-1565
35.64	35.81	40.07	40.14	9.66	9.96	-6.396	6.252	0.018	-0.058	-0.043	-819	115	1180	-807	-1111	71	2041	-1472
39.82	40.27	40.05	40.37	9.65	10.03	-6.393	6.252	0.045	-0.058	-0.045	-851	137	1181	-773	-1222	81	2044	-1429
44.53	44.48	40.09	40.37	9.64	10.05	-6.382	6.249	0.090	-0.061	-0.053	-872	167	1185	-723	-1356	86	2068	-1358
49.64	49.72	40.04	40.59	9.60	10.13	-6.372	6.252	0.195	-0.056	-0.054	-860	229	1181	-668	-1550	84	2081	-2310
54.26	54.57	40.04	40.40	9.55	10.14	-6.358	6.252	0.459	-0.006	-0.047	-749	373	1138	-519	-1815	51	2124	-1155
54.62	55.78	39.90	39.26	9.48	9.88	-6.317	6.245	0.781	0.110	-0.047	-559	567	1103	-297	-1964	-62	2307	-2599

Table E.2: Column Test Data - Test 1 - PT

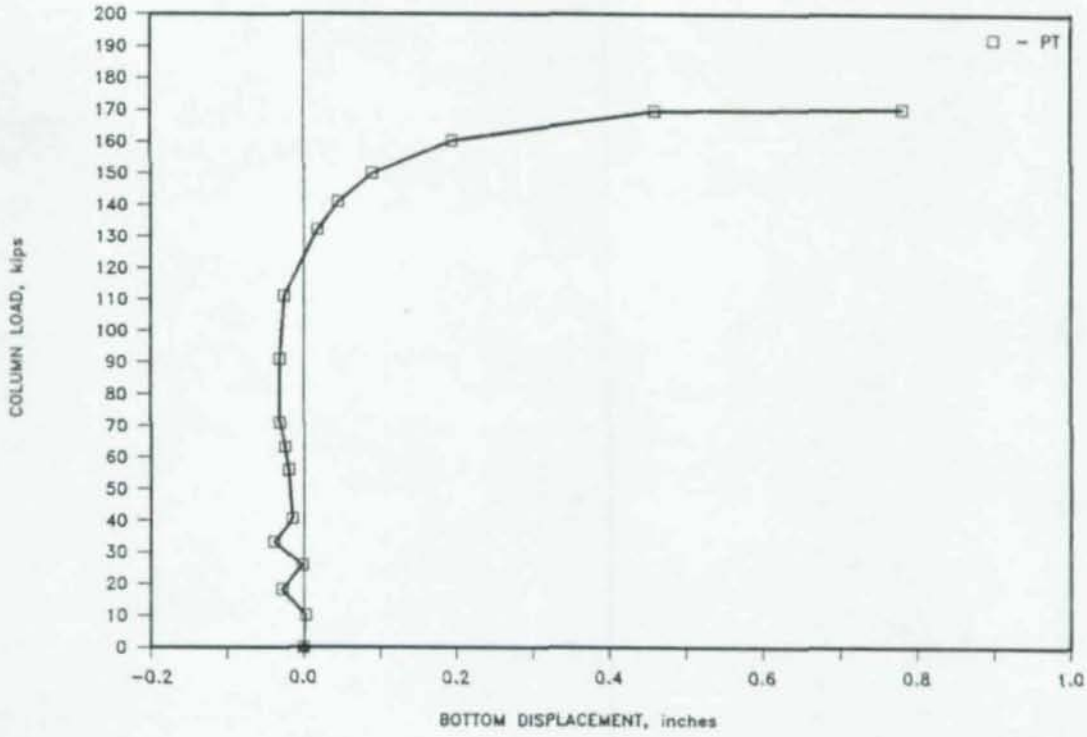

Figure E.1: P_{col} vs. δ_{bottom} – Test 1 – PT

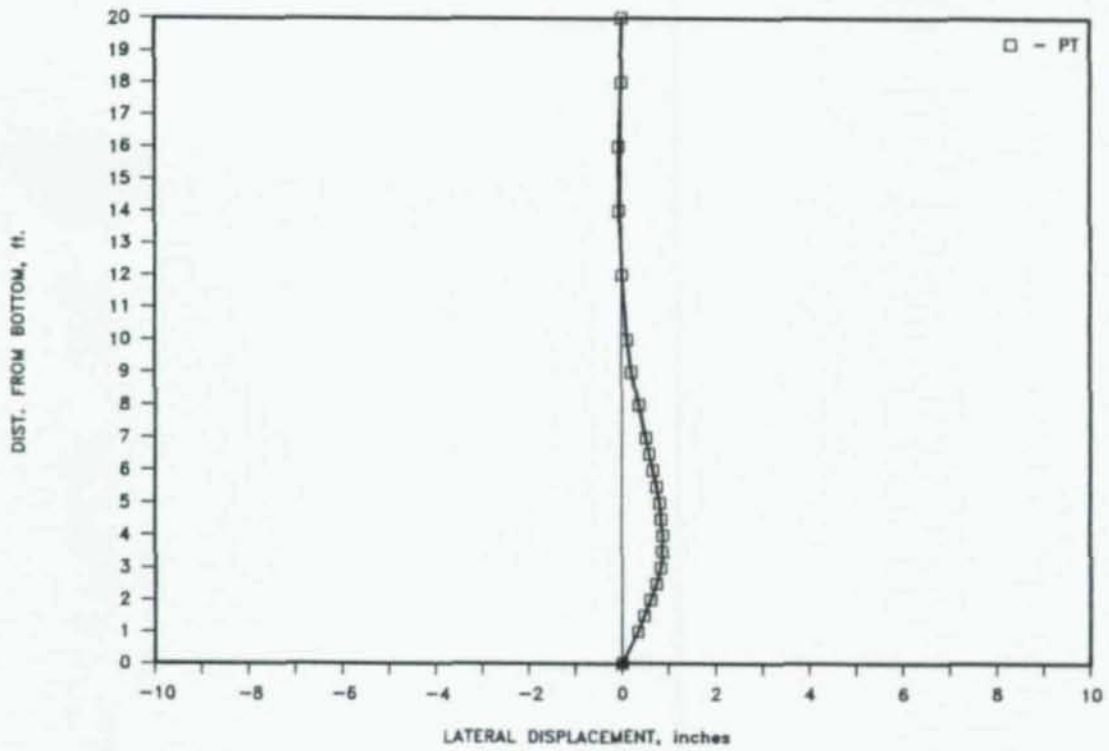

Figure E.2: Buckled Shape Under 10-kip Load - Test 1 - PT

EAST LOAD (kips)	WEST LOAD (kips)	SOUTH LOAD (kips)	NORTH LOAD (kips)	SOUTH REACT. (kips)	NORTH REACT. (kips)	SOUTH SLOPE (milli-radians)	NORTH SLOPE (milli-radians)	BOTT. DISP. (inches)	MIDL. DISP. (inches)	TOP DISP. (inches)	NORTH AXIAL (micro inch/inch)	NORTH TRANS (micro inch/inch)	NORTH TOP (micro inch/inch)	NORTH BOTT. (micro inch/inch)	SOUTH AXIAL (micro inch/inch)	SOUTH TRANS (micro inch/inch)	SOUTH TOP (micro inch/inch)	SOUTH BOTT. (micro inch/inch)
0.00	0.00	0.00	0.00	0.00	0.00	0.000	0.000	0.000	0.000	0.000	0	0	0	0	0	0	0	0
5.02	5.18	-0.21	-0.16	-0.02	-0.06	-0.059	-0.036	-0.010	0.000	0.002	-76	42	1	39	-72	55	-19	46
5.02	5.06	-0.20	4.95	-0.04	1.32	-0.041	0.021	0.003	0.006	-0.006	-156	-56	15	6	-91	-37	29	15
5.10	5.14	-0.20	9.97	-0.05	2.62	-0.034	0.590	0.022	0.011	-0.016	-237	-149	48	-39	-110	-117	73	-10
5.09	5.06	-0.22	20.07	-0.08	5.15	-0.041	2.245	0.069	0.019	-0.048	-412	-427	267	-260	-139	-298	168	-82
4.98	5.10	4.96	19.95	1.20	5.10	-0.079	2.274	0.059	0.016	-0.039	-432	-524	323	-301	-210	-385	253	-149
4.92	5.06	9.95	19.98	2.42	5.08	-0.854	2.288	0.041	0.015	-0.026	-452	-623	365	-339	-280	-480	309	-207
5.03	5.16	19.88	19.98	4.85	5.04	-2.454	2.306	0.005	0.009	-0.000	-475	-826	453	-409	-408	-683	437	-294
5.19	5.61	19.94	10.11	4.90	2.55	-2.998	1.616	-0.036	0.002	0.027	-314	-633	319	-232	-366	-520	336	-226
5.16	5.23	19.97	-0.30	4.94	-0.17	-3.098	0.618	-0.089	-0.012	0.057	-134	-351	209	-108	-344	-348	272	-145
5.07	5.18	10.08	-0.29	2.50	-0.13	-1.942	0.533	-0.058	-0.007	0.035	-88	-165	130	-24	-209	-183	169	-63
5.07	5.14	0.04	-0.28	0.05	-0.07	-0.558	0.529	-0.020	-0.002	0.008	-43	40	31	67	-63	34	4	61
0.01	0.00	0.05	-0.27	0.06	-0.09	-0.372	0.426	-0.010	-0.004	0.003	34	2	33	26	10	-13	24	29

Table E.3: Connection Test Data - Test 2 - TT

EAST LOAD (kips)	WEST LOAD (kips)	SOUTH LOAD (kips)	NORTH LOAD (kips)	SOUTH REACT. (kips)	NORTH REACT. (kips)	SOUTH SLOPE (milli-radians)	NORTH SLOPE (milli-radians)	BOTT. DISP. (inches)	MIDL. DISP. (inches)	TOP DISP. (inches)	NORTH AXIAL (micro inch/inch)	NORTH TRANS (micro inch/inch)	NORTH TOP (micro inch/inch)	NORTH BOTT. (micro inch/inch)	SOUTH AXIAL (micro inch/inch)	SOUTH TRANS (micro inch/inch)	SOUTH TOP (micro inch/inch)	SOUTH BOTT. (micro inch/inch)
0.00	0.00	0.00	0.00	0.00	0.00	0.000	0.000	0.000	0.000	0.000	27	-129	61	9	3	-144	152	67
5.02	5.14	-0.17	-0.01	-0.03	0.01	0.010	-0.004	-0.006	0.001	0.003	-49	-88	58	49	-68	-90	132	133
5.03	5.29	10.00	10.13	2.43	2.56	-0.874	0.625	-0.010	0.006	0.010	-254	-475	206	-132	-248	-449	384	-34
5.04	5.31	20.00	20.18	4.86	5.05	-2.448	2.128	-0.008	0.009	0.012	-459	-897	449	-419	-420	-830	616	-220
4.92	4.94	29.95	30.51	7.30	7.61	-4.052	3.726	-0.010	0.007	0.011	-577	-1413	826	-635	-513	-1353	963	-335
4.99	4.90	40.02	40.40	9.76	10.04	-5.673	5.332	-0.026	0.001	0.009	-572	-2096	1141	-777	-511	-2096	1289	-445
14.94	14.99	38.74	39.13	9.43	9.72	-5.721	5.339	-0.048	-0.010	0.010	-722	-2041	1194	-655	-627	-2026	1284	-342
24.84	25.06	39.97	40.08	9.74	9.95	-5.718	5.339	-0.047	-0.012	0.018	-936	-2084	1325	-606	-820	-1981	1318	-281
35.03	34.79	40.01	40.44	9.75	10.04	-5.718	5.339	-0.073	-0.022	0.026	-1150	-2110	1444	-538	-983	-1879	1331	-197
39.92	39.83	39.98	40.77	9.76	10.11	-5.718	5.339	-0.107	-0.029	0.033	-1258	-2152	1525	-516	-1051	-1812	1343	-152
45.45	44.73	39.98	40.61	9.78	10.04	-5.718	5.339	-0.182	-0.038	0.053	-1357	-2253	1599	-485	-1093	-1707	1329	-91
48.79	49.52	40.01	40.65	9.81	10.04	-5.745	5.560	-0.325	-0.059	0.083	-1393	-2490	1701	-487	-1073	-1555	1324	-31
52.53	53.43	38.78	40.48	9.53	9.95	-5.742	5.560	-0.543	-0.087	0.135	-1368	-2835	1801	-497	-961	-1272	1199	80
51.14	51.83	39.85	40.44	9.85	9.91	-5.745	5.560	-0.716	-0.116	0.179	-1183	-3170	1827	-536	-875	-1208	1154	60
51.43	52.30	38.63	40.57	9.59	9.91	-5.535	5.638	-0.995	-0.176	0.220	-1001	-3568	1902	-525	-667	-890	972	128

Table E.4: Column Test Data - Test 2 - TT

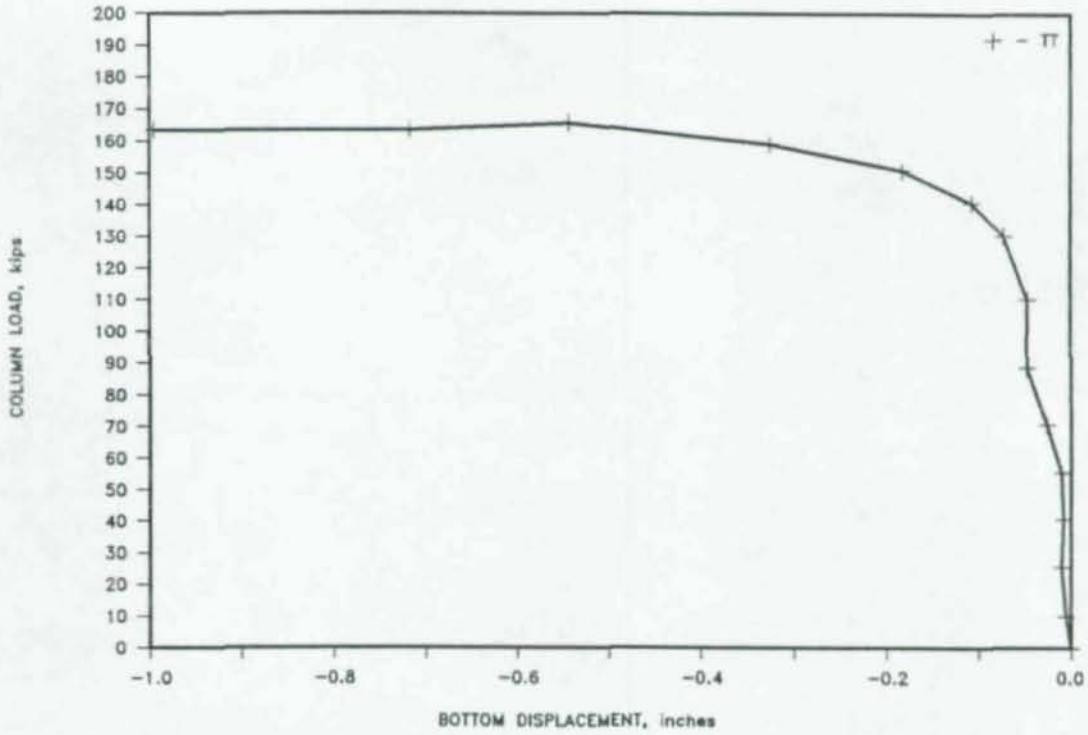

Figure E.3: P_{col} vs. δ_{bottom} – Test 2 – TT

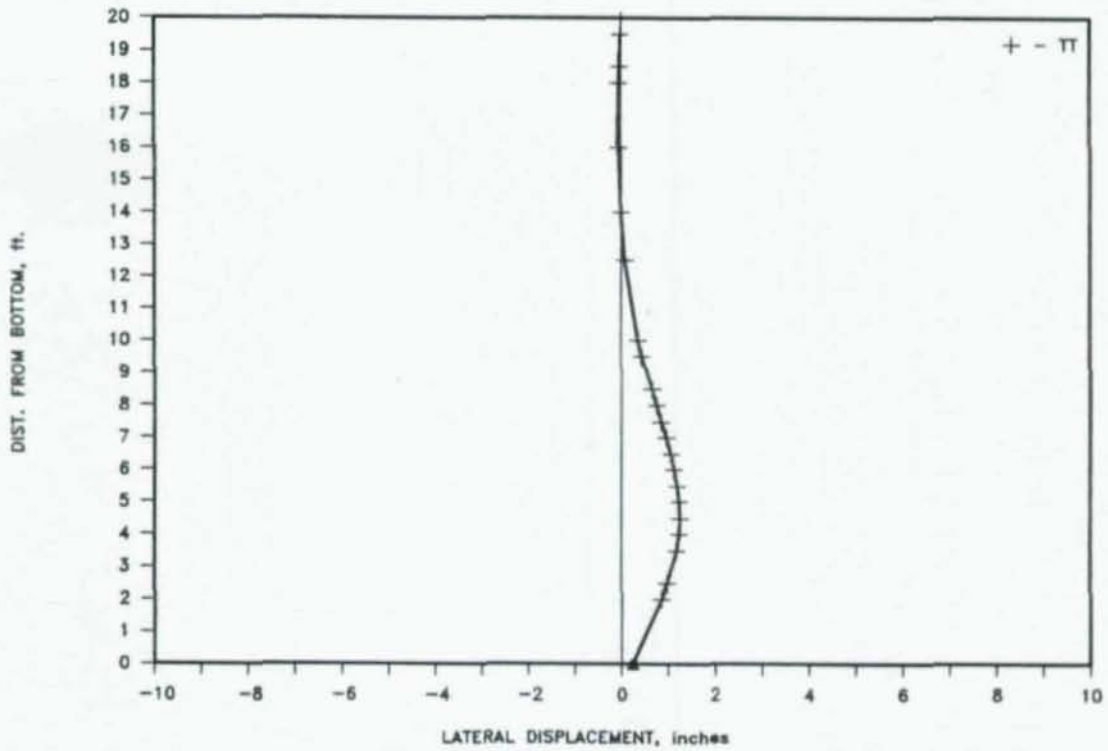

Figure E.4: Buckled Shape Under 10-kip Load - Test 2 - TT

EAST LOAD (kips)	WEST LOAD (kips)	SOUTH LOAD (kips)	NORTH LOAD (kips)	SOUTH REACT. (kips)	NORTH REACT. (kips)	SOUTH SLOPE (milli-radians)	NORTH SLOPE	BOTT. DISP. (inches)	MIDL. DISP. (inches)	TOP DISP. (inches)	NORTH AXIAL	NORTH TRANS	NORTH TOP	NORTH BOTT.	SOUTH AXIAL	SOUTH TRANS	SOUTH TOP	SOUTH BOTT.
											(micro inch/inch)							
0.00	0.00	0.00	0.00	0.00	0.00	0.000	0.000	0.000	0.000	0.000	0	0	0	0	0	0	0	0
5.09	4.99	-0.01	0.00	0.01	0.00	0.021	0.007	-0.000	0.001	0.007	-67	10	41	18	-70	13	-66	-9
5.11	5.34	0.00	4.95	-0.02	1.30	0.107	0.462	0.021	0.010	-0.006	-128	1	55	44	-73	22	8	-20
5.07	5.10	-0.01	9.99	-0.02	2.62	0.107	1.176	0.064	0.018	-0.036	-200	-18	177	72	-55	44	10	-15
5.02	5.07	0.00	20.03	-0.03	5.15	0.103	3.030	0.168	0.030	-0.113	-359	-63	555	-20	-14	92	-15	-112
5.07	5.07	5.04	20.00	1.18	5.10	-0.282	4.004	0.155	0.030	-0.100	-361	-53	590	-49	-76	84	27	-232
4.99	5.03	10.05	19.94	2.39	5.06	-1.105	4.007	0.130	0.030	-0.077	-355	-37	607	-41	-145	71	68	-479
5.01	5.06	20.02	20.04	4.81	5.06	-2.740	4.007	0.055	0.030	-0.006	-325	12	628	-24	-292	48	244	-978
5.23	5.22	20.04	10.68	4.86	2.71	-2.950	2.536	-0.035	0.016	0.065	-190	49	351	66	-320	17	206	-947
5.04	5.07	20.01	-0.02	4.87	-0.05	-2.967	1.126	-0.159	-0.005	0.150	-4	112	110	9	-376	-43	233	-938
4.94	4.87	10.15	0.00	2.46	-0.01	-1.800	0.998	-0.106	-0.001	0.101	-11	82	31	-22	-245	-27	90	-687
5.10	4.99	0.27	0.00	0.09	0.00	-0.272	0.991	-0.031	0.001	0.030	-50	30	94	-55	-89	11	-3	-455
0.01	0.03	0.28	-0.01	0.10	-0.01	-0.224	0.927	-0.030	-0.000	0.029	14	15	60	-78	-16	3	40	-436

Table E.5: Connection Test Data - Test 3 - PS

EAST LOAD (kips)	WEST LOAD (kips)	SOUTH LOAD (kips)	NORTH LOAD (kips)	SOUTH REACT. (kips)	NORTH REACT. (kips)	SOUTH SLOPE (milli-radians)	NORTH SLOPE (milli-radians)	BOTT. DISP. (inches)	MIDL. DISP. (inches)	TOP DISP. (inches)	NORTH AXIAL (micro inch/inch)	NORTH TRANS (micro inch/inch)	NORTH TOP (micro inch/inch)	NORTH BOTT. (micro inch/inch)	SOUTH AXIAL (micro inch/inch)	SOUTH TRANS (micro inch/inch)	SOUTH TOP (micro inch/inch)	SOUTH BOTT. (micro inch/inch)
0.00	0.00	0.00	0.00	0.00	0.00	0.000	0.000	0.000	0.000	0.000	14	15	60	-78	-16	3	40	-436
5.03	4.77	-0.19	0.01	-0.05	0.02	0.052	-0.096	0.001	0.003	-0.009	-56	28	54	-58	-84	13	-35	-433
5.12	4.85	9.95	9.97	2.36	2.56	-1.232	0.796	0.007	0.012	-0.001	-169	40	196	56	-215	16	115	-682
4.98	4.67	19.99	20.22	4.72	5.12	-2.771	2.533	0.022	0.021	0.003	-291	46	522	-19	-331	25	324	-996
5.02	4.80	30.07	30.13	7.16	7.54	-4.527	4.213	0.032	0.025	0.003	-406	58	965	-174	-451	42	587	-1371
5.00	4.79	40.33	40.37	9.64	10.05	-6.310	5.964	0.034	0.025	0.003	-525	68	1450	-473	-577	58	877	-1813
15.14	14.71	40.08	40.01	9.58	9.96	-6.379	5.972	0.036	0.025	0.003	-653	100	1500	-403	-727	87	898	-1818
25.12	24.85	40.10	40.00	9.58	9.97	-6.379	5.968	0.094	0.025	0.003	-787	136	1552	-353	-904	108	920	-1796
34.84	34.48	39.98	40.04	9.53	9.97	-6.365	5.968	0.155	0.031	0.003	-910	175	1598	-295	-1111	125	969	-1773
44.73	44.62	39.99	40.28	9.50	10.07	-6.248	5.940	0.299	0.054	0.002	-1003	237	1630	-202	-1412	145	1115	-1751
50.01	49.90	40.34	40.36	9.53	10.07	-6.251	5.936	0.569	0.113	-0.042	-947	317	1681	-72	-1688	132	1263	-1747

Table E.6: Column Test Data - Test 3 - PS

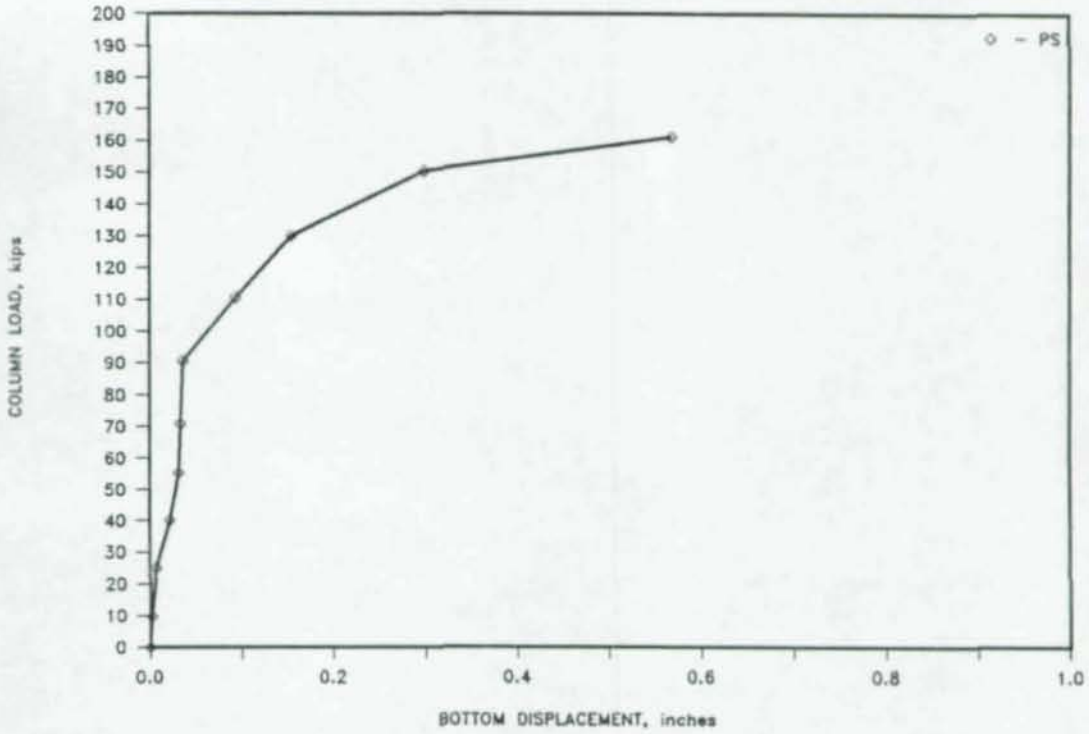

Figure E.5: P_{col} vs. δ_{bottom} – Test 3 – PS

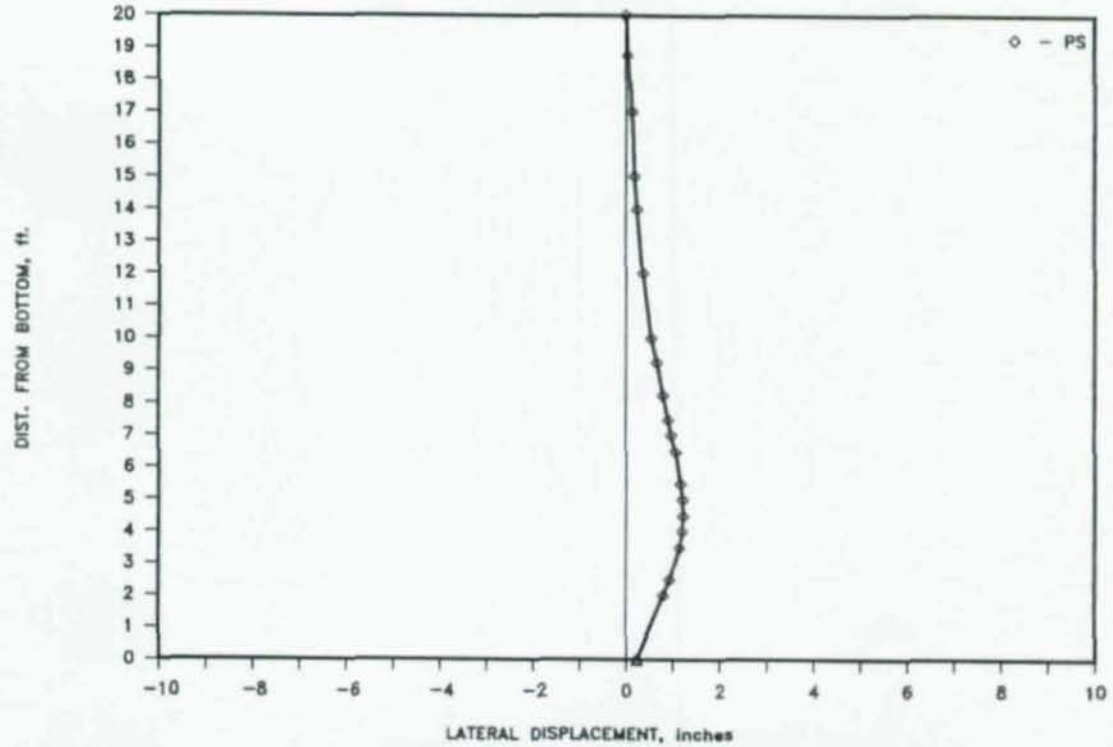

Figure E.6: Buckled Shape Under 10-kip Load - Test 3 - PS

EAST LOAD (kips)	WEST LOAD (kips)	SOUTH LOAD (kips)	NORTH LOAD (kips)	SOUTH REACT. (kips)	NORTH REACT. (kips)	SOUTH SLOPE (milli-radians)	NORTH SLOPE	BOTT. DISP. (inches)	MIDL. DISP. (inches)	TOP DISP. (inches)	NORTH AXIAL	NORTH TRANS	NORTH TOP	NORTH BOTT.	SOUTH AXIAL	SOUTH TRANS	SOUTH TOP	SOUTH BOTT.
											(micro inch/inch)							
0.00	0.00	0.00	0.00	0.00	0.00	0.000	0.000	0.000	0.000	0.000	0	0	0	0	0	0	0	0
5.02	4.85	-0.28	-0.02	-0.06	0.04	0.055	-0.281	-0.001	0.001	-0.005	-61	37	-107	17	-76	28	63	48
5.17	5.06	-0.29	4.96	-0.07	1.22	0.103	-0.281	0.037	0.008	-0.026	-144	-183	-27	-5	-82	-54	91	12
5.25	5.11	-0.27	9.96	-0.08	2.45	0.107	-0.277	0.083	0.018	-0.057	-232	-408	105	-107	-78	-100	103	-3
5.12	4.85	-0.27	20.15	-0.07	4.90	0.103	-0.234	0.179	0.026	-0.132	-380	-845	469	-317	-61	-142	93	-10
5.06	4.86	4.87	19.98	1.15	4.83	-0.186	-0.234	0.159	0.026	-0.110	-370	-933	496	-350	-156	-357	213	-338
5.01	4.89	9.89	19.95	2.36	4.82	-0.713	-0.231	0.128	0.026	-0.078	-360	-995	501	-380	-240	-591	325	-505
5.15	4.94	19.83	19.91	4.76	4.79	-2.368	-0.220	0.054	0.026	-0.008	-340	-1099	502	-412	-356	-1100	644	-717
5.06	5.09	19.62	10.74	4.72	2.60	-2.640	-0.227	-0.022	0.019	0.059	-189	-693	258	-128	-345	-975	571	-637
5.13	5.01	19.41	-0.05	4.68	0.01	-2.647	-0.234	-0.127	0.004	0.134	2	-125	-32	107	-357	-827	495	-550
5.12	4.84	10.09	-0.03	2.41	0.02	-1.528	-0.234	-0.087	0.006	0.092	5	-77	-43	115	-198	-613	365	-265
5.09	4.89	-0.05	-0.03	0.02	0.03	-0.062	-0.234	0.001	0.005	0.000	-23	-31	20	147	36	-114	127	253
0.07	0.59	0.01	-0.03	0.03	0.03	-0.062	-0.234	0.001	0.002	0.002	34	-60	112	132	105	-138	175	203

Table E.7: Connection Test Data - Test 4 - TS

EAST LOAD (kips)	WEST LOAD (kips)	SOUTH LOAD (kips)	NORTH LOAD (kips)	SOUTH REACT. (kips)	NORTH REACT. (kips)	SOUTH SLOPE (milli-radians)	NORTH SLOPE	BOTT. DISP. (inches)	MIDL. DISP. (inches)	TOP DISP. (inches)	NORTH				SOUTH			
											AXIAL	TRANS	TOP	BOTT.	AXIAL	TRANS	TOP	BOTT.
											(micro inch/inch)							
0.00	0.00	0.00	0.00	0.00	0.00	0.000	0.000	0.000	0.000	0.000	34	-60	112	132	105	-138	175	203
5.00	5.10	-0.14	0.01	-0.03	-0.01	0.003	0.000	0.002	0.001	-0.001	-31	-33	34	156	28	-108	154	272
5.00	4.94	9.97	9.95	2.40	2.39	-0.867	0.128	0.014	0.017	0.009	-186	-556	208	-19	-184	-660	444	-294
5.10	4.93	20.11	20.19	4.84	4.83	-2.423	0.789	0.014	0.022	0.012	-334	-1058	484	-357	-370	-1171	745	-729
5.04	4.99	30.29	30.23	7.35	7.26	-4.017	2.114	0.026	0.024	0.011	-396	-1667	836	-580	-364	-1829	1053	-935
5.03	4.84	40.23	40.30	9.82	9.71	-5.900	2.440	0.042	0.024	0.001	-306	-2616	1165	-793	-209	-2628	1401	-1103
14.93	15.22	40.13	40.25	9.79	9.70	-5.904	2.440	0.044	0.024	0.001	-432	-2578	1192	-745	-387	-2604	1482	-1041
24.99	24.78	40.15	40.22	9.80	9.69	-5.917	2.440	0.071	0.026	0.001	-560	-2541	1247	-689	-565	-2593	1533	-981
34.82	34.96	40.25	40.18	9.82	9.69	-5.917	2.440	0.121	0.026	-0.009	-682	-2484	1314	-642	-759	-2613	1638	-923
44.79	44.93	40.10	39.95	9.76	9.64	-5.935	2.440	0.325	0.047	-0.037	-737	-2336	1350	-569	-909	-2814	1814	-849
50.28	49.58	40.11	39.49	9.72	9.61	-5.921	2.440	0.824	0.134	-0.120	-605	-1932	1253	-456	-779	-3380	2070	-795

Table E.8: Column Test Data - Test 4 - TS

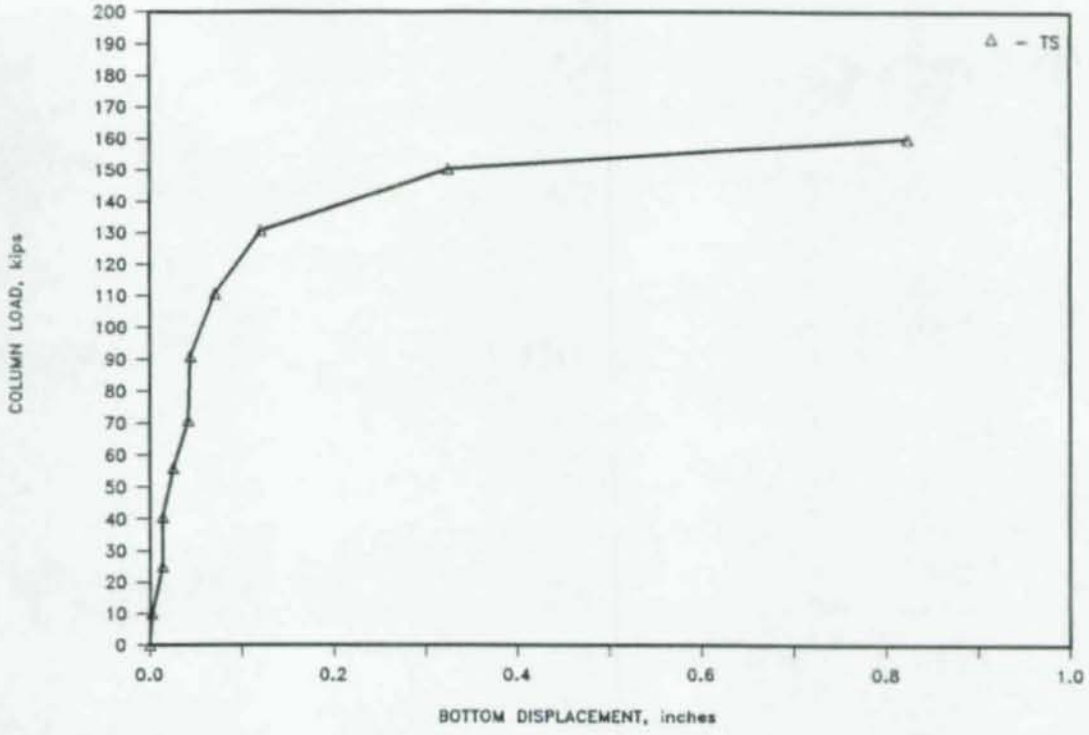

Figure E.7: P_{col} vs. δ_{bottom} – Test 4 – TS

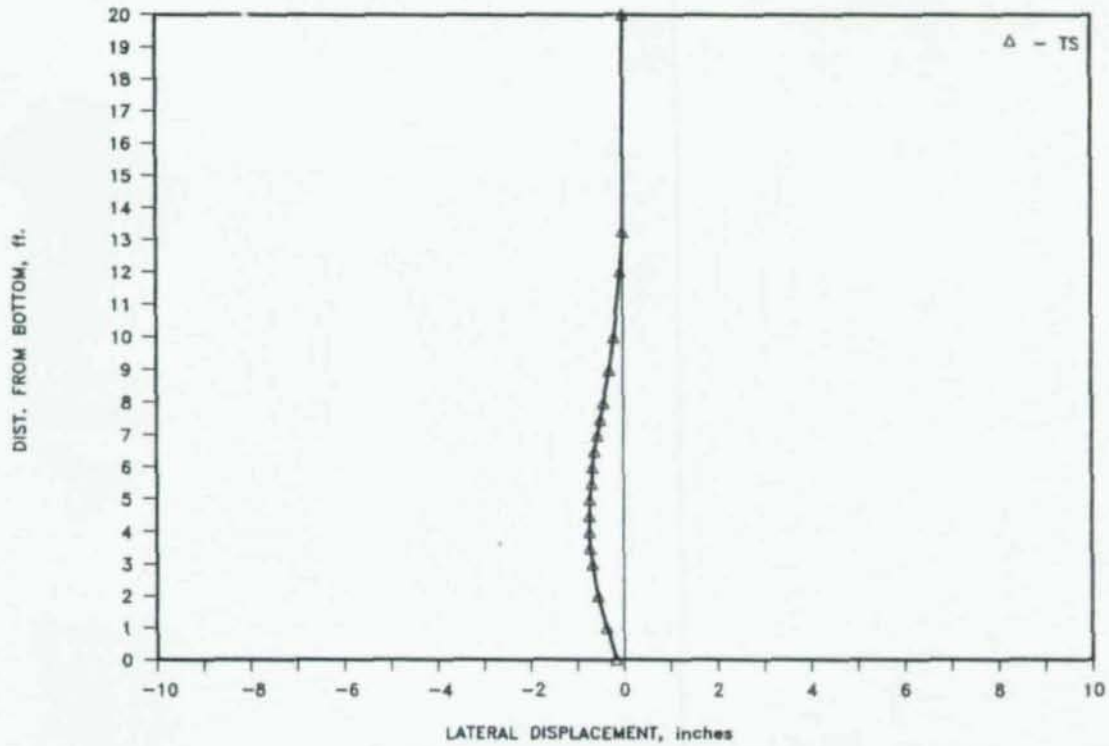

Figure E.8: Buckled Shape Under 10-kip Load – Test 4 – TS